

A Multi-responsive System based on Intramolecular B←O=P Lewis Acid-base Pairs

Supporting Information

Yu Wang,^a Kanglei Liu,^a Pangkuan Chen,^a Xiaodong Yin,^a Tai Peng,^{*b} Javed Iqbal,^c
and Nan Wang^{*a}

^a Key Laboratory of Cluster Science of Ministry of Education, Beijing Key Laboratory of Photoelectronic/Electrophotonic Conversion Materials, School of Chemistry and Chemical Engineering, Beijing Institute of Technology, Beijing, P. R. China

^b School of Materials Science & Engineering, Jiamusi University

^c Department of Chemistry, University of Agriculture, Faisalabad, Faisalabad, Pakistan

Table of Contents

S1. Experimental Details

S2. TD-DFT Calculation Data

S3. NMR and HRMS Spectra

S4. X-ray Crystallographic Data

S1. Experimental Details

General Information

Materials were purchased from J&K Scientific Ltd. and used without further purification. Solvents were dried using standard procedures prior to use. Compound **B**¹ was synthesized according to previously reported procedures. ¹H, ¹³C and ¹¹B NMR spectra were recorded on a Bruker Avance 400 MHz, or 700 MHz spectrometer. ¹¹B NMR spectra were acquired with boron-free quartz NMR tubes and the spectra were referenced externally to BF₃·Et₂O ($\delta = 0$). ³¹P NMR spectra were recorded on a Bruker Avance 400 MHz spectrometer and the spectra were referenced to 85% H₃PO₄ as an external standard. UV-visible absorption spectra were obtained on an Agilent Cary 300 UV-Vis spectrophotometer. Fluorescence spectra were recorded on an Edinburgh Instruments FLS980 spectrophotometer. Fluorescent quantum efficiencies were determined using a Hamamatsu Quantaurus-QY spectrometer (C11347). High-resolution mass spectra (HRMS) were obtained from an Agilent Q-TOF 6520 LC-MS spectrometer. The powder X-ray diffraction (PXRD) patterns were recorded on a Bruker D8 Advance diffractometer.

DFT calculations were performed with the Gaussian 09 program.² Geometry optimizations and vertical excitations were calculated by means of hybrid density functional M062X with the basis set of 6-31G(d). The input files and orbital representations were generated with Gaussview 5.0 (isovalue =0.03). Excitation data were calculated using TD-DFT (M062X functional and 6-31G* basis).³ The resulting structures were confirmed to be stationary points through vibrational frequency analysis.

X-ray single crystals were obtained on a Bruker D8 X-ray single crystal Venture diffractometer using Mo K α radiation ($\lambda = 0.71073 \text{ \AA}$) at 180K for all compounds. SAINT5.0 and SADABS programs⁴ are used for the reduction and absorption correction of crystal data. The resolution and refinement of the crystal structure are obtained on the SHELXTL-97 software⁵, using the direct or Patterson methods. All non-hydrogen source coordinates are obtained by using the differential Fourier method and the least square method. Then the geometric method and the difference value are used. The hydrogen atom coordinates were obtained by Fourier method, and the crystal structure was obtained. The CCDC numbers of 2093720 (B2), and 2170359 (B3) are deposited.

Synthesis of B1-1. 1-Bromo-4-fluoro-2-iodobenzene (1.20 g, 4.00 mmol), carbazole (0.17 g, 1.00 mmol), potassium carbonate (0.55 g, 4.00 mmol) were added to DMF (50 mL) solution. And heat the reaction mixture to 150 °C for 24 hours. After reaction completion, add the mixture to brine (40 mL). Extract the mixture with CH₂Cl₂ (3 × 15 mL). Concentrate the combined extract under reduced pressure. The crude product was purified with chromatography on silica using PE/DCM (10/1, v/v) to give white solid. Yield: 0.14 g, 31%. ¹H NMR (400 MHz, CDCl₃) δ 8.13 (d, J = 7.7 Hz, 2H), 8.09 (d, J = 2.4 Hz, 1H), 7.84 (d, J = 8.5 Hz, 1H), 7.50 – 7.35 (m, 5H), 7.31 (t, J = 7.3 Hz, 2H); ¹³C NMR (101 MHz, CDCl₃) δ 140.55, 138.64, 137.66, 133.72, 128.49, 128.18, 126.39, 123.78, 120.69, 120.61, 109.62, 102.08. ESI-MS. Calcd. for C₁₈H₁₂BrIN([M+H])⁺: m/z 447.9192. Found: m/z 447.9188.

Synthesis of B1-2. A solution of Pd(PPh₃)₄ (0.12 g, 0.10 mmol),

diphenylphosphine (0.22 mL, 2.00 mmol), **B1-1** (0.90 g, 2.00 mmol), Et₃N (0.32 mL, 2.24 mmol) and 50 mL of anhydrous toluene was heated at 80 °C for 12 hours under nitrogen. After cooling to RT, the solvent was removed under reduced pressure and the solid residue was dissolved in H₂O (30 mL) and extracted with CH₂Cl₂. Then the organic layer was dried over Na₂SO₄. CH₂Cl₂ was evaporated under reduced pressure. The crude product was purified with chromatography on silica using PE/DCM (12/1, v/v) to give white solid. Yield: 0.77 g, 76%. ¹H NMR (400 MHz, *d*-DMSO) δ 8.18 (d, J = 7.7 Hz, 2H), 7.98 (dd, J = 8.4, 3.8 Hz, 1H), 7.66 (dd, J = 8.4, 2.3 Hz, 1H), 7.50 – 7.21 (m, 16H), 6.85 (t, J = 2.3 Hz, 1H). ¹³C NMR (101 MHz, DMSO) δ 140.59, 140.44, 139.09, 136.54, 134.74, 134.71, 134.63, 133.60, 133.39, 131.24, 129.49, 129.11, 129.04, 128.21, 126.84, 126.54, 126.27, 122.86, 120.51, 120.49, 109.50. ESI-MS. Calcd. for C₃₀H₂₂BrNP([M+H]⁺): m/z 506.0668. Found: m/z 506.0664.

Synthesis of B1. Compound **B1-2** (0.51 g, 1.00 mmol) was placed in a dry round bottom flask with a side-arm under N₂, and anhydrous THF (30 mL) was added to the flask. The solution was cooled to -78 °C and *n*-BuLi (1.60 M in hexane, 0.69 mL, 1.10 mmol) was added and stirred for 1 hour at -78 °C. Mes₂BF (0.34 g, 1.25 mmol) was added at -78 °C and the solution was slowly warmed up to room temperature and stirred overnight. The reaction was then quenched by addition of H₂O and an excess amount of H₂O₂ (10 mL, 30 wt. % in H₂O) was added. The THF was removed from the resulting mixture on a rotary evaporator, and the mixture was then extracted with diethyl ether and the organic phase washed with first water and then brine, before drying over anhydrous MgSO₄. The mixture was filtered and the solvent was removed from the

filtrate under vacuum. Purification by column chromatography (PE: EA=10:1) gave a white solid. Yield: 0.30 g, 43%. ^1H NMR (400 MHz, CDCl_3) δ 8.14 (d, $J = 7.7$ Hz, 2H), 7.96 (dd, $J = 8.1, 2.1$ Hz, 1H), 7.75 (dd, $J = 9.1, 1.8$ Hz, 1H), 7.65 (d, $J = 8.0$ Hz, 1H), 7.59 – 7.49 (m, 2H), 7.46 – 7.26 (m, 14H), 6.62 (s, 4H), 2.23 (s, 6H), 1.97 (s, 12H). ^{13}C NMR (101 MHz, CDCl_3) δ 140.84, 140.54, 136.11, 135.95, 134.99, 134.82, 133.99, 133.23, 133.21, 132.37, 132.25, 131.04, 129.90, 129.14, 128.80, 128.67, 127.61, 126.57, 126.05, 125.52, 125.35, 123.47, 120.50, 120.13, 109.47, 25.01, 20.83. ESI-MS. Calcd. for $\text{C}_{48}\text{H}_{43}\text{BNNaOP}([\text{M}+\text{Na}]^+)$: m/z 714.3068. Found: m/z 714.3073.

Synthesis of B2-1. A solution of $\text{Pd}(\text{PPh}_3)_4$ (0.12 g, 0.10 mmol), diphenylphosphine (0.22 mL, 2.00 mmol), **B** (0.65 g, 2.00 mmol), Et_3N (0.32 mL, 2.24 mmol) and 50 mL of anhydrous toluene was heated at 80 °C for 12 hours under nitrogen. After cooling to RT, the solvent was removed under reduced pressure and the solid residue was dissolved in H_2O (30 mL) and extracted with CH_2Cl_2 . Then the organic layer was dried over Na_2SO_4 . CH_2Cl_2 was evaporated under reduced pressure. The crude product was purified with chromatography on silica using PE/DCM (5/1, v/v) to give white solid. Yield: 0.53 g, 69%. ^1H NMR (400 MHz, CD_2Cl_2) δ 7.49 – 7.15 (m, 11H), 6.56 (dd, $J = 8.8, 3.1$ Hz, 1H), 6.04 (t, $J = 3.3$ Hz, 1H), 2.67 (s, 6H). ^{13}C NMR (101 MHz, CD_2Cl_2) δ 150.10, 138.84, 138.73, 136.93, 136.81, 134.51, 134.31, 133.33, 133.29, 129.32, 128.96, 128.89, 119.08, 119.07, 115.85, 115.55, 114.61, 40.25. ESI-MS. Calcd. for $\text{C}_{20}\text{H}_{20}\text{BrNP}([\text{M}+\text{H}]^+)$: m/z 384.0511. Found: m/z 384.0505.

Synthesis of B2. Compound **B2-1** (0.38 g, 1.00 mmol) was placed in a dry round bottom flask with a side-arm under N_2 , and anhydrous THF (30 mL) was added to the

flask. The solution was cooled to -78 °C and *n*-BuLi (1.60 M in hexane, 0.69 mL, 1.10 mmol) was added and stirred for 1 hour at -78 °C. Mes₂BF (0.34 g, 1.25 mmol) was added at -78 °C and the solution was slowly warmed up to room temperature and stirred overnight. The reaction was then quenched by addition of H₂O and an excess amount of H₂O₂ (10 mL, 30 wt. % in H₂O) was added. The THF was removed from the resulting mixture on a rotary evaporator, and the mixture was then extracted with diethyl ether and the organic phase washed with first water and then brine, before drying over anhydrous MgSO₄. The mixture was filtered and the solvent was removed from the filtrate under vacuum. Purification by column chromatography (PE: DCM=10:1) gave a white solid. Yield: 0.28 g, 49%. ¹H NMR (400 MHz, CDCl₃) δ 7.48 (m, 3H), 7.40 – 7.26 (m, 8H), 6.89 (d, J = 8.4 Hz, 1H), 6.76 (d, J = 11.1 Hz, 1H), 6.53 (s, 4H), 2.93 (s, 6H), 2.18 (s, 6H), 1.89 (s, 12H). ¹³C NMR (101 MHz, CDCl₃) δ 149.62, 149.47, 147.73, 140.84, 134.12, 134.07, 133.90, 132.49, 132.46, 132.40, 132.29, 129.63, 129.43, 128.77, 128.53, 128.41, 118.00, 117.97, 110.81, 110.63, 40.78, 24.80, 20.99. ESI-MS. Calcd. for C₃₈H₄₂BNOP([M+H])⁺: m/z 570.3092. Found: m/z 570.3108.

Synthesis of B3. Compound **B2-1** (0.38 g, 1.00 mmol) was placed in a dry round bottom flask with a side-arm under N₂, and anhydrous THF (30 mL) was added to the flask. The solution was cooled to -78 °C and *n*-BuLi (1.60 M in hexane, 0.69 mL, 1.10 mmol) was added and stirred for 1 hour at -78 °C. (OMe-Mes)₂BF (0.38 g, 1.25 mmol) was added at -78 °C and the solution was slowly warmed up to room temperature and stirred overnight. The reaction was then quenched by addition of H₂O and an excess amount of H₂O₂ (10 mL, 30 wt. % in H₂O) was added. The THF was removed from the

resulting mixture on a rotary evaporator, and the mixture was then extracted with diethyl ether and the organic phase washed with first water and then brine, before drying over anhydrous MgSO₄. The mixture was filtered and the solvent was removed from the filtrate under vacuum. Purification by column chromatography (PE: EA=4:1) gave a white solid. Yield: 0.31 g, 51%. ¹H NMR (400 MHz, CDCl₃) δ 7.52 – 7.43 (m, 2H), 7.44 – 7.28 (m, 9H), 6.87 (d, J = 8.0 Hz, 1H), 6.72 (d, J = 10.2 Hz, 1H), 6.29 (s, 4H), 3.73 (s, 6H), 2.92 (s, 6H), 1.92 (s, 12H). ¹³C NMR (101 MHz, CDCl₃) δ 157.63, 149.49, 149.34, 142.65, 134.18, 134.01, 132.07, 132.04, 132.00, 131.90, 131.17, 130.30, 130.12, 129.28, 128.33, 128.20, 116.91, 112.94, 112.14, 111.96, 99.99, 54.65, 40.48, 24.75. ESI-MS. Calcd. for C₃₈H₄₂BNO₃P([M+H])⁺: m/z 602.2990. Found: m/z 602.2982.

Synthesis of B4-I. A solution of Pd(PPh₃)₄ (0.12 g, 0.10 mmol), Di-o-tolylphosphine (0.65 g, 2.00 mmol), **B** (0.65 g, 2.00 mmol), K₂CO₃ (0.55 g, 4.00 mmol) and 50 mL of anhydrous toluene was heated at 110 °C for 24 hours under nitrogen. After cooling to RT, the solvent was removed under reduced pressure and the solid residue was dissolved in H₂O (30 mL) and extracted with CH₂Cl₂. Then the organic layer was dried over Na₂SO₄. CH₂Cl₂ was evaporated under reduced pressure. The crude product was purified with chromatography on silica using PE/DCM (5/1, v/v) to give white solid. Yield: 0.56 g, 68%. ¹H NMR (400 MHz, CD₂Cl₂) δ 7.39 (dd, J = 8.8, 4.2 Hz, 1H), 7.34 – 7.17 (m, 4H), 7.09 (t, J = 7.1 Hz, 2H), 6.77 (dd, J = 7.4, 4.0 Hz, 2H), 6.57 (dd, J = 8.8, 3.1 Hz, 1H), 6.04 (t, J = 3.2 Hz, 1H), 2.65 (s, 6H), 2.42 (s, 6H). ¹³C NMR (101 MHz, CD₂Cl₂) δ 150.31, 143.31, 143.04, 137.59, 137.49, 135.06, 134.94,

133.60, 133.37, 133.34, 130.50, 130.45, 129.32, 126.55, 119.03, 116.57, 116.26, 114.66, 40.26, 21.43, 21.21. ESI-MS. Calcd. for $C_{22}H_{24}BrNP([M+H])^+$: m/z 412.0824. Found: m/z 412.0807.

Synthesis of B4. Compound **B4-1** (0.41 g, 1.00 mmol) was placed in a dry round bottom flask with a side-arm under N_2 , and anhydrous THF (30 mL) was added to the flask. The solution was cooled to -10 °C and *n*-BuLi (1.60 M in hexane, 0.69 mL, 1.10 mmol) was added and stirred for 1.5 hours at -10 °C. Mes₂BF (0.34 g, 1.25 mmol) was added at -10 °C and the solution was slowly warmed up to room temperature and stirred overnight. The reaction was then quenched by addition of H₂O and an excess amount of H₂O₂ (10 mL, 30 wt. % in H₂O) was added. The THF was removed from the resulting mixture on a rotary evaporator, and the mixture was then extracted with diethyl ether and the organic phase washed with first water and then brine, before drying over anhydrous MgSO₄. The mixture was filtered and the solvent was removed from the filtrate under vacuum. Purification by column chromatography (PE: EA=10:1) gave a white solid. Yield: 0.19 g, 32%. ¹H NMR (400 MHz, CD₂Cl₂) δ 7.55 – 7.33 (m, 5H), 7.24 – 7.08 (m, 3H), 7.04 (t, J = 7.3 Hz, 2H), 6.97 (d, J = 8.4 Hz, 1H), 6.55 (s, 4H), 2.98 (s, 6H), 2.21 (s, 6H), 2.18 (s, 6H), 1.85 (s, 12H). ¹³C NMR (101 MHz, CD₂Cl₂) δ 149.50, 149.35, 140.88, 140.77, 140.30, 133.96, 133.78, 133.42, 133.29, 133.18, 132.60, 132.57, 131.62, 131.51, 128.85, 128.75, 128.60, 127.77, 127.58, 125.83, 125.70, 118.08, 110.93, 110.75, 40.45, 24.50, 21.44, 21.40, 20.43. ESI-MS. Calcd. for $C_{40}H_{46}BNOP([M+H])^+$: m/z 598.3405. Found: m/z 598.3396.

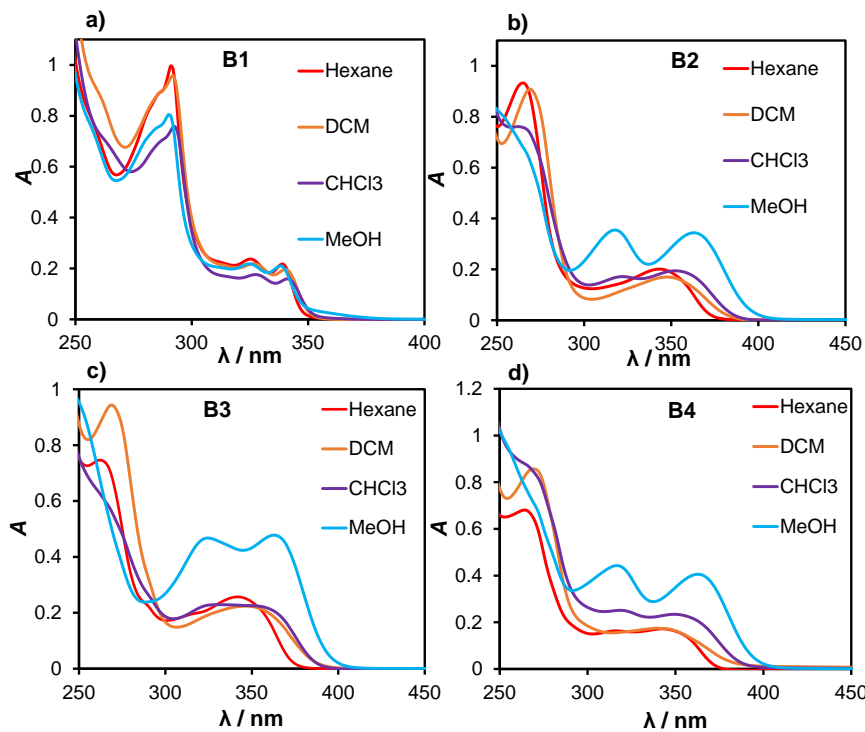


Figure S1. UV-Visible absorption spectra of **B1**(a), **B2**(b), **B3**(c) and **B4**(d) in various solvents.

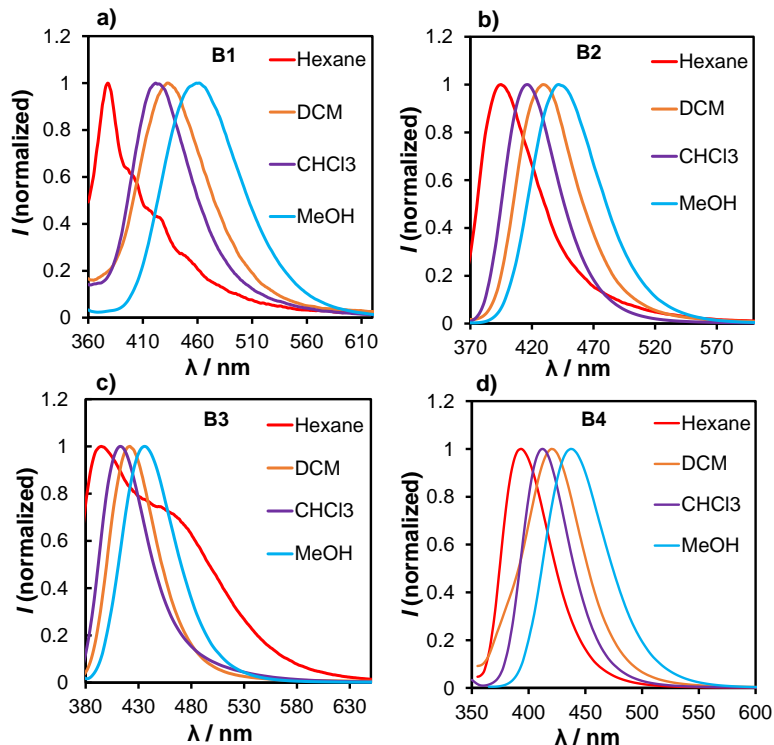


Figure S2. Fluorescence spectra of **B1**(a), **B2**(b), **B3**(c) and **B4**(d) in various solvents.

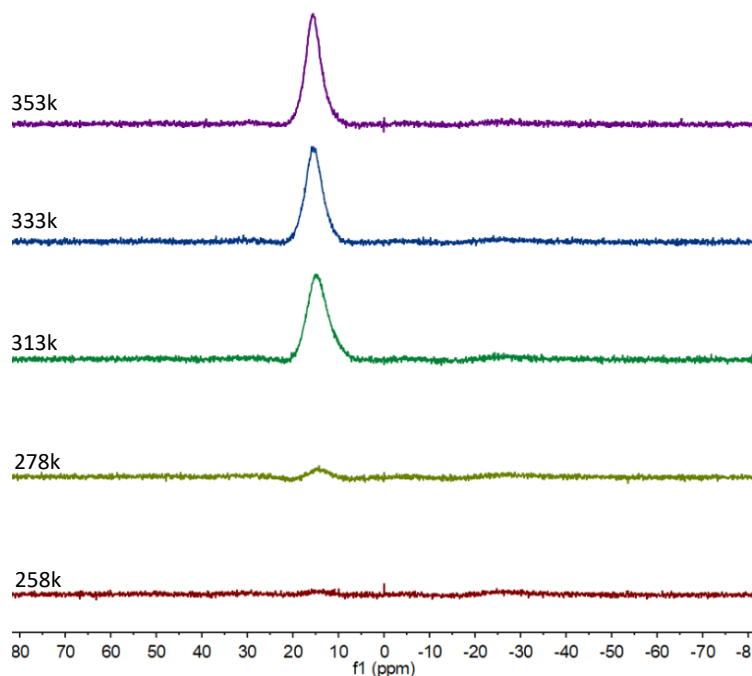


Figure S3. VT ^{11}B NMR spectra of **B1** in toluene- d_8 .

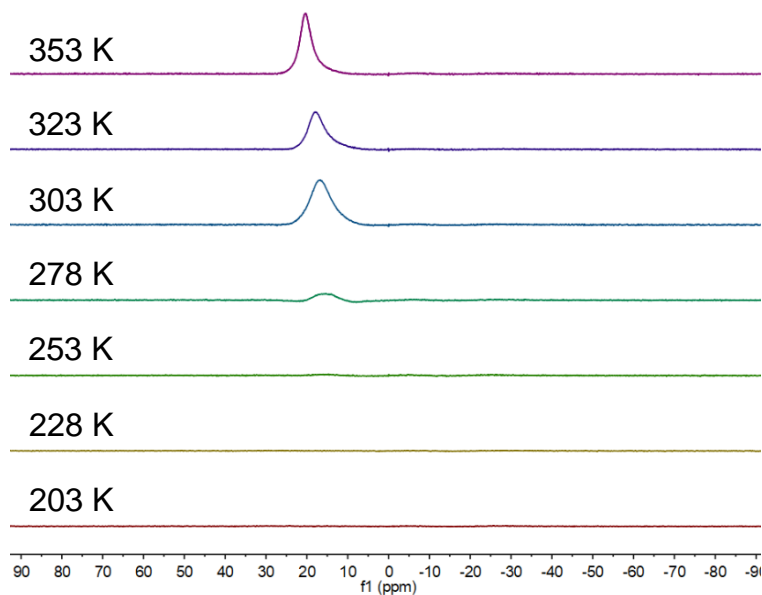


Figure S4. VT ^{11}B NMR spectra of **B2** in toluene- d_8 .

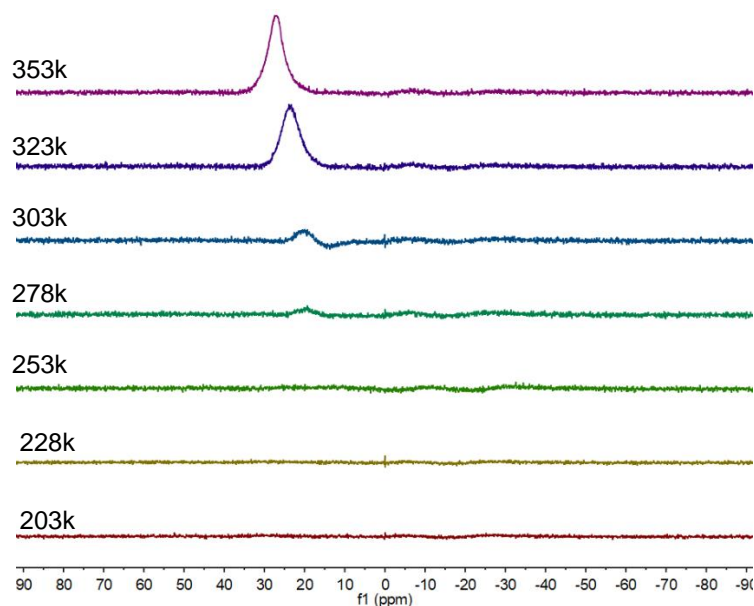


Figure S5. VT ^{11}B NMR spectra of **B3** in toluene- d_8 .

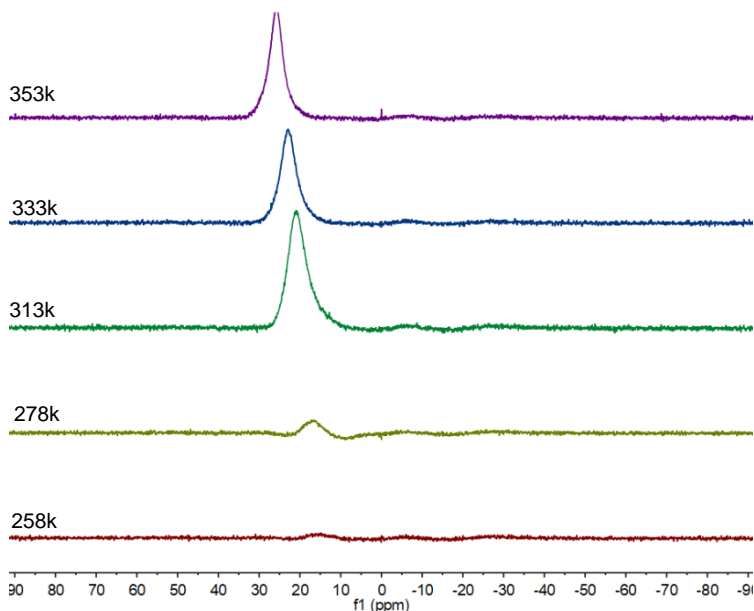


Figure S6. VT ^{11}B NMR spectra of **B4** in toluene- d_8 .

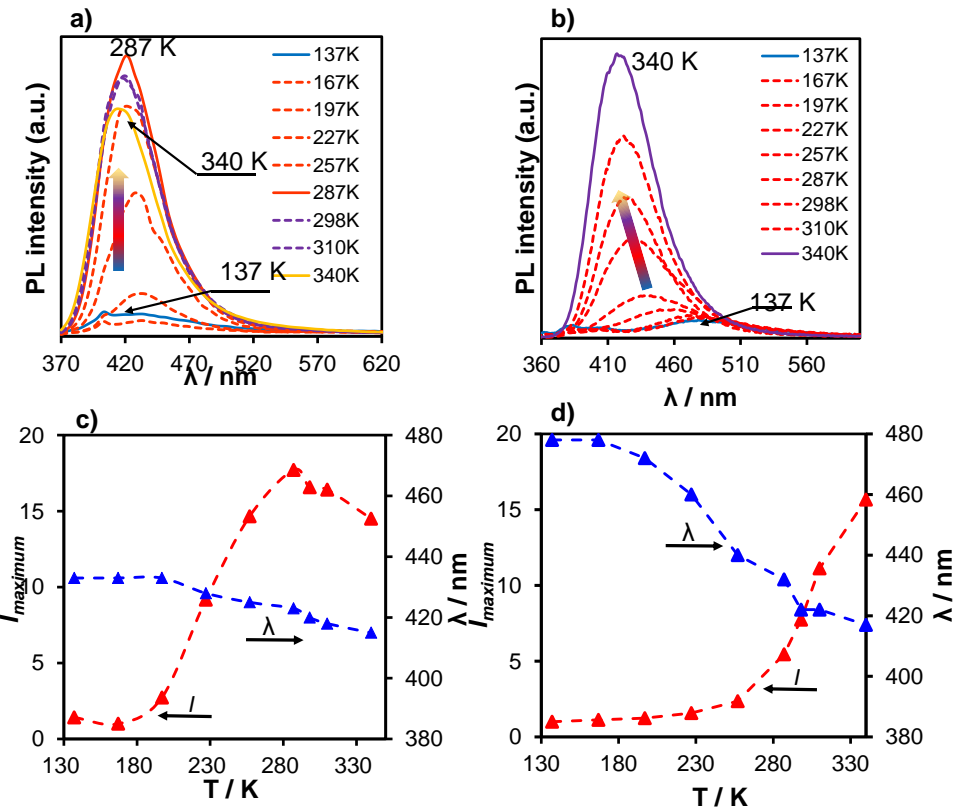


Figure S7. VT emission spectra of **B3** (a) and **B4** (b) recorded in 2-Me-THF ($c = 1 \times 10^{-5} \text{ M}$); Plots of emission intensity ratio of maximum emission to minimum emission intensity at 130 K (I) (red dashed line) and wavelengths (λ) (blue dashed line) versus temperature for **B3** (c) and **B4** (d);

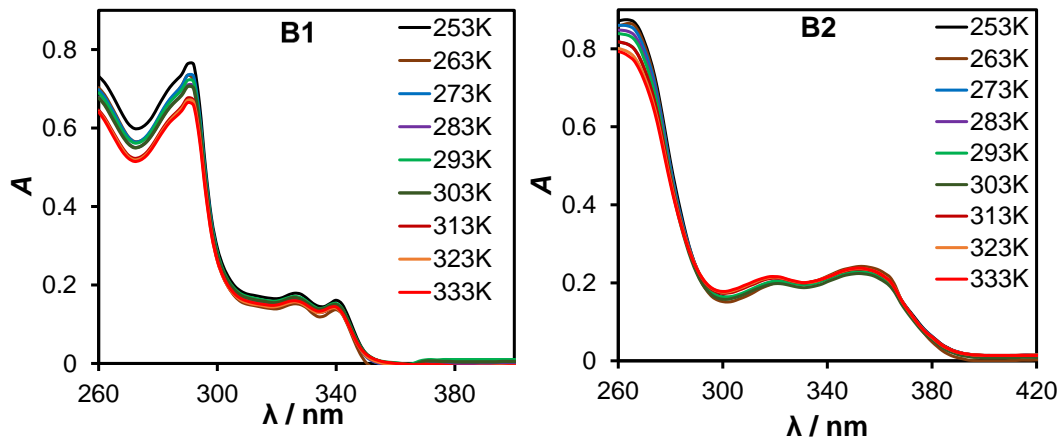


Figure S8. VT UV-Vis spectra of **B1** (left) and **B2** (right) recorded in CH_3Cl ($c = 3 \times 10^{-5} \text{ M}$).

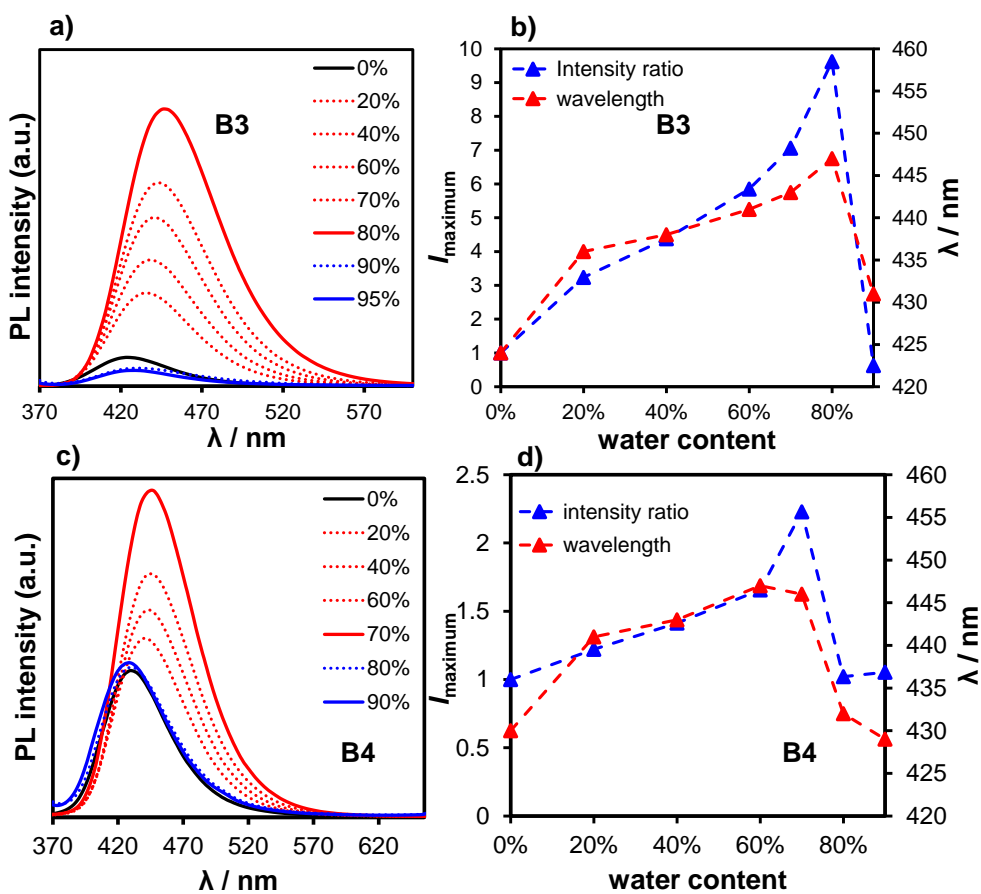


Figure S9. Impact of water content in fluorescence spectra for **B3** (a) and **B4** (c) in THF (1×10^{-5} M) solution; Plots of emission intensity ratio of maximum emission to minimum emission intensity (blue dashed line) and wavelengths (red dashed line) versus water content for **B3** (b) and **B4** (d).

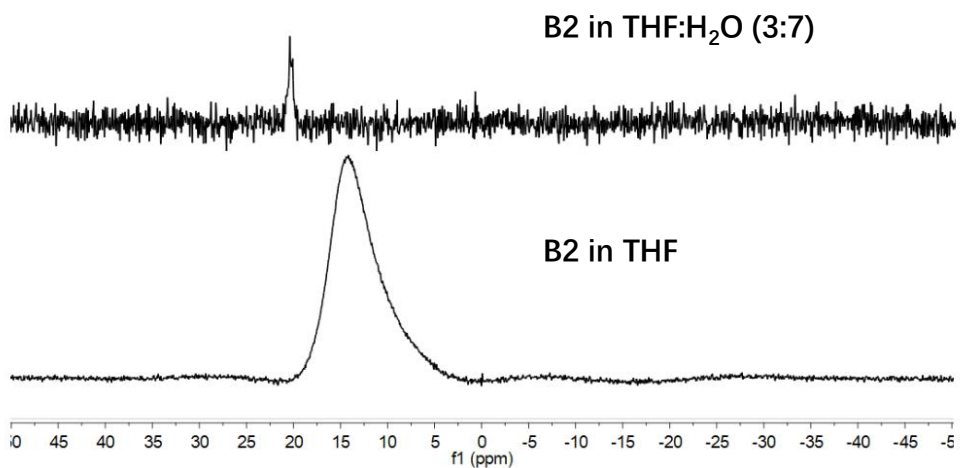


Figure S10. ^{11}B NMR spectra of **B2** in the solvent mixture of THF and water (3:7) (top) and in THF (bottom) (700 MHz, 298 K).

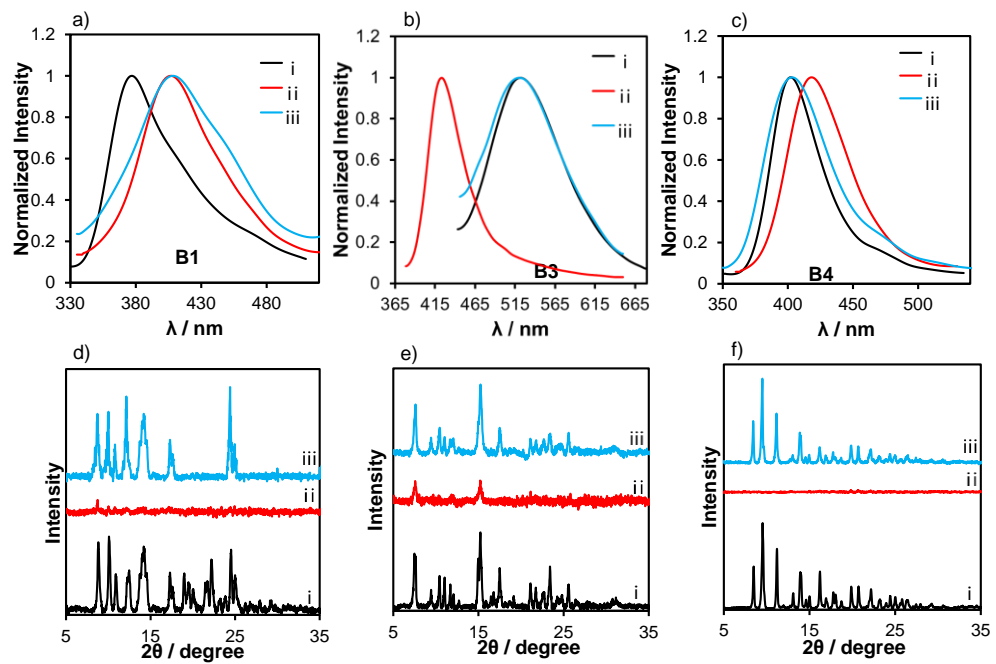


Figure S11. Normalized solid state emission spectra and powder XRD patterns of **B1** (a, d), **B3** (b, e) and **B4** (c, f) under different conditions as (i) pristine crystalline solid; (ii) ground powder; (iii) solid by MeOH vapour treatment.

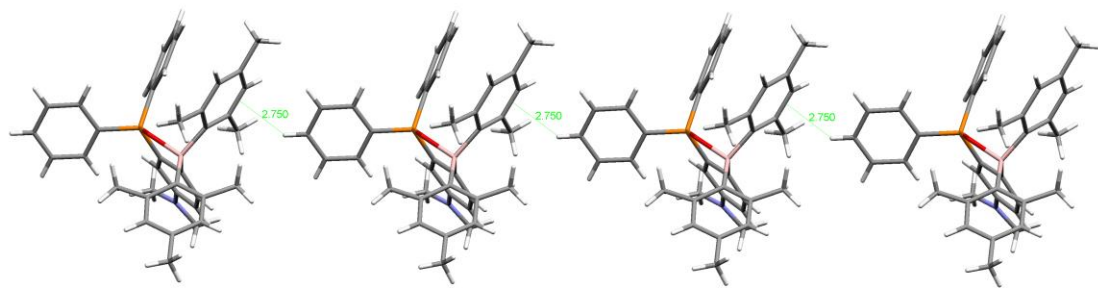


Figure S12. Relative orientations of **B2** molecules and the C-H \cdots π interactions in the crystal lattice.

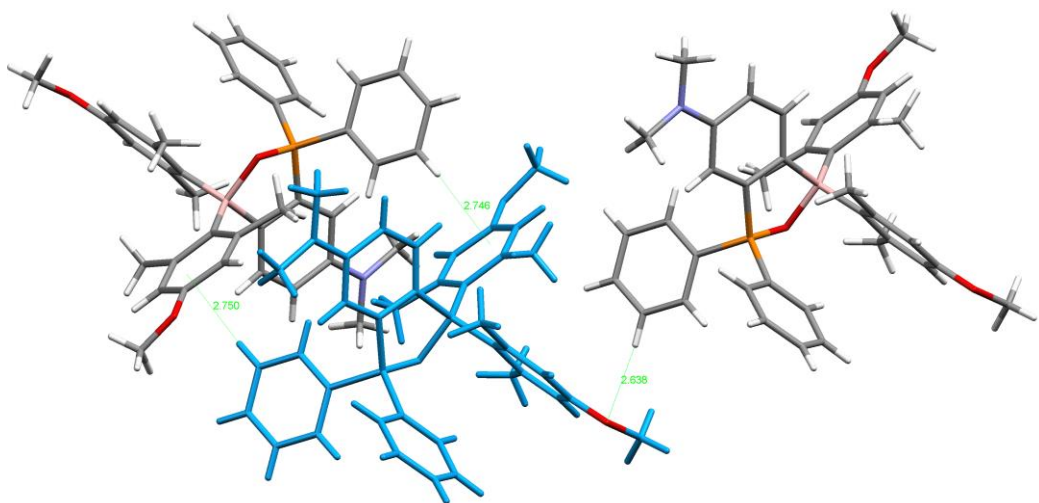


Figure S13. Relative orientations of **B3** molecules and the C-H $\cdots\pi$ interactions in the crystal lattice.

S2. TD-DFT Calculation Data

Table S1. TD-DFT calculated electronic transitions for **B1** along with their corresponding excitation energies and oscillator strengths.

Compound	Spin State	Transition Configuration	Excitation Energy [nm (eV)]	Oscillator Strength
B1	S1	HOMO-6→LUMO+1 (3%)	283.36 (4.38)	0.0523
		HOMO→LUMO (14%)		
		HOMO→LUMO+1 (50%)		
		HOMO→LUMO+2 (7%)		
		HOMO→LUMO+3 (3%)		
		HOMO→LUMO+4 (3%)		
		HOMO→LUMO+5 (7%)		
	S2	HOMO-4→LUMO+7 (8%)	281.42 (4.41)	0.0785
		HOMO-1→LUMO+3 (20%)		
		HOMO→LUMO+1 (3%)		
		HOMO→LUMO+3 (58%)		
	S3	HOMO-2→LUMO+1 (3%)	266.65 (4.65)	0.0650
		HOMO-1→LUMO (22%)		
		HOMO-1→LUMO+1 (20%)		
		HOMO-1→LUMO+5 (2%)		
		HOMO→LUMO (30%)		
		HOMO→LUMO+1 (2%)		
		HOMO→LUMO+4 (5%)		
		HOMO→LUMO+5 (3%)		
	S4	HOMO-3→LUMO+1 (9%)	263.58 (4.70)	0.0030
		HOMO-2→LUMO (23%)		
		HOMO-2→LUMO+1 (49%)		
		HOMO→LUMO (11%)		
	S5	HOMO-2→LUMO (3%)	262.78 (4.72)	0.0039
		HOMO-2→LUMO+1 (2%)		
		HOMO-1→LUMO (5%)		
		HOMO-1→LUMO+1 (32%)		
		HOMO-1→LUMO+2 (3%)		
		HOMO-1→LUMO+4 (5%)		
		HOMO→LUMO (29%)		
		HOMO→LUMO+1 (12%)		

Table S2. Primary orbitals which contribute to the calculated transitions of **B1** (iso = 0.03).

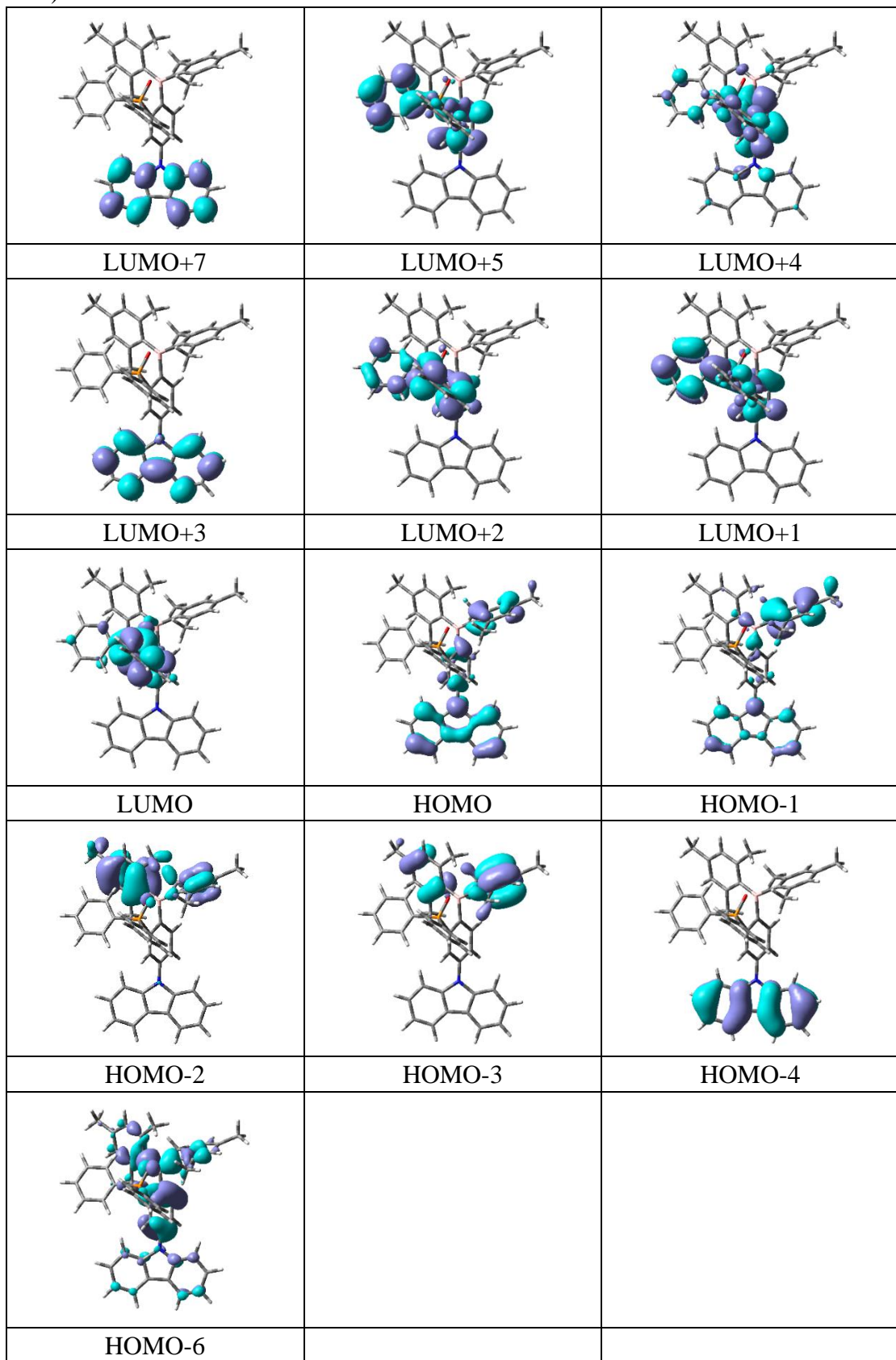


Table S3. TD-DFT calculated electronic transitions for **B2-closed** along with their corresponding excitation energies and oscillator strengths.

Compound	Spin State	Transition Configuration	Excitation Energy [nm (eV)]	Oscillator Strength
B2-closed	S1	HOMO→LUMO (25%)	287.35 (4.31)	0.0674
		HOMO→LUMO+1 (33%)		
		HOMO→LUMO+2 (3%)		
		HOMO→LUMO+3 (18%)		
		HOMO→LUMO+4 (7%)		
	S2	HOMO-2→LUMO (2%)	270.34 (4.59)	0.0245
		HOMO-1→LUMO (2%)		
		HOMO-1→LUMO+1 (2%)		
		HOMO→LUMO (64%)		
		HOMO→LUMO+1 (18%)		
		HOMO→LUMO+3 (4%)		
	S3	HOMO-3→LUMO+1 (4%)	263.88 (4.70)	0.0078
		HOMO-2→LUMO+1 (60%)		
		HOMO-2→LUMO+2 (3%)		
		HOMO-1→LUMO+1 (18%)		
		HOMO-1→LUMO+2 (2%)		
		HOMO→LUMO+1 (3%)		
		HOMO→LUMO+2 (2%)		
	S4	HOMO-3→LUMO (2%)	253.46 (4.89)	0.0041
		HOMO-2→LUMO (71%)		
		HOMO-2→LUMO+3 (5%)		
		HOMO-1→LUMO (10%)		
	S5	HOMO-4→LUMO+1 (4%)	250.70 (4.95)	0.0054
		HOMO-2→LUMO (3%)		
		HOMO-2→LUMO+1 (4%)		
		HOMO-1→LUMO (48%)		
		HOMO-1→LUMO+1 (20%)		
		HOMO-1→LUMO+3 (5%)		
		HOMO→LUMO (2%)		

Table S4. Primary orbitals which contribute to the calculated transitions of **B2-closed** (iso = 0.03).

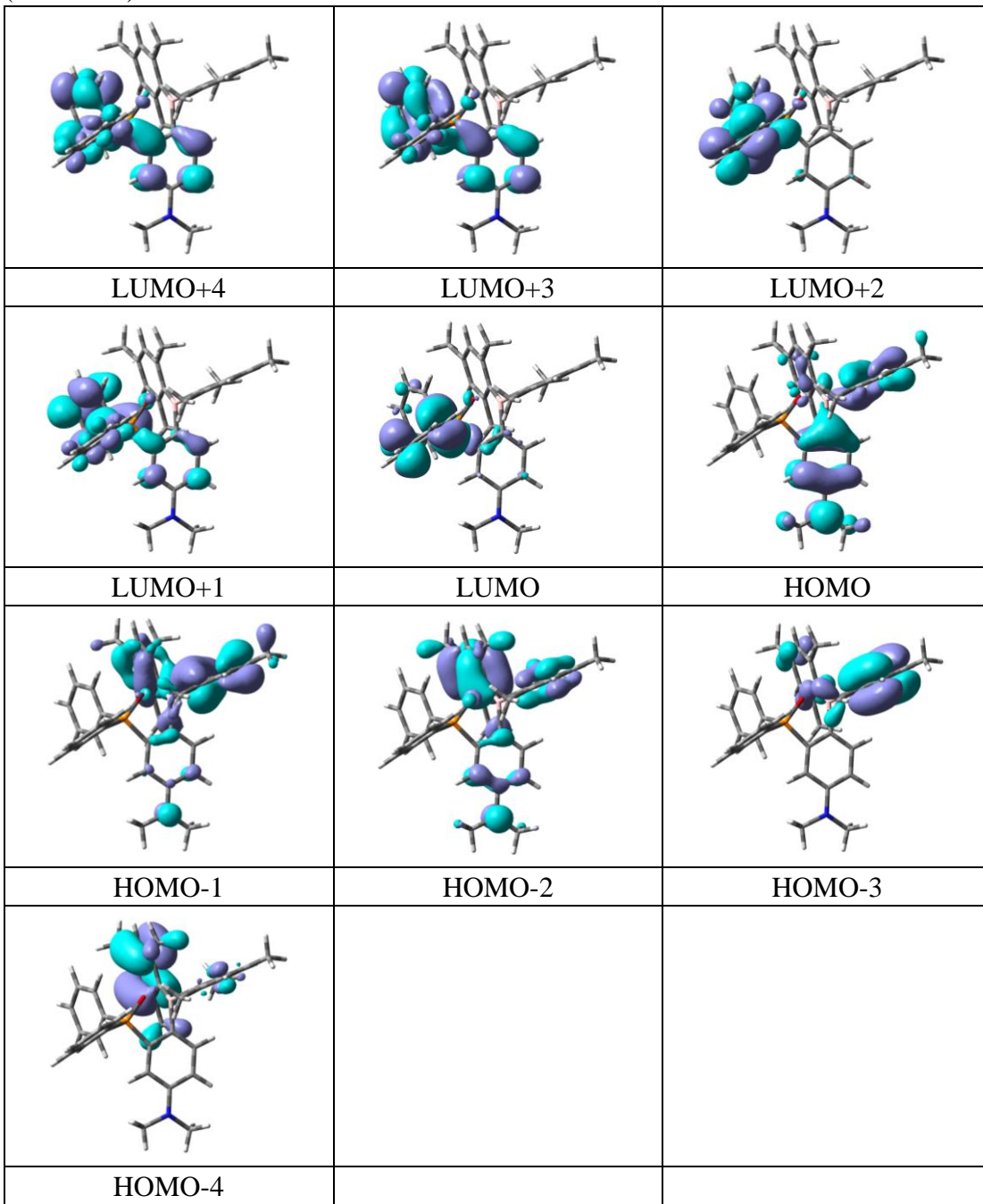


Table S5. TD-DFT calculated electronic transitions for **B3-closed** along with their corresponding excitation energies and oscillator strengths.

Compound	Spin State	Transition Configuration	Excitation Energy [nm (eV)]	Oscillator Strength
B3-closed	S1	HOMO→LUMO (99%)	411.19(3.02)	0.0042
	S2	HOMO-1→LUMO (93%)	384.46 (3.22)	0.0138
		HOMO-1→LUMO+1 (5%)		
	S3	HOMO→LUMO+1 (97%)	375.62 (3.30)	0.0232

	S4	HOMO-2→LUMO (82%) HOMO-1→LUMO+1 (15%)	369.15 (3.36)	0.0022
	S5	HOMO-2→LUMO (14%)	365.67 (3.39)	0.0098
		HOMO-1→LUMO (6%)		
		HOMO-1→LUMO+1 (79%)		

Table S6. Primary orbitals which contribute to the calculated transitions of **B3-closed** (iso = 0.03).

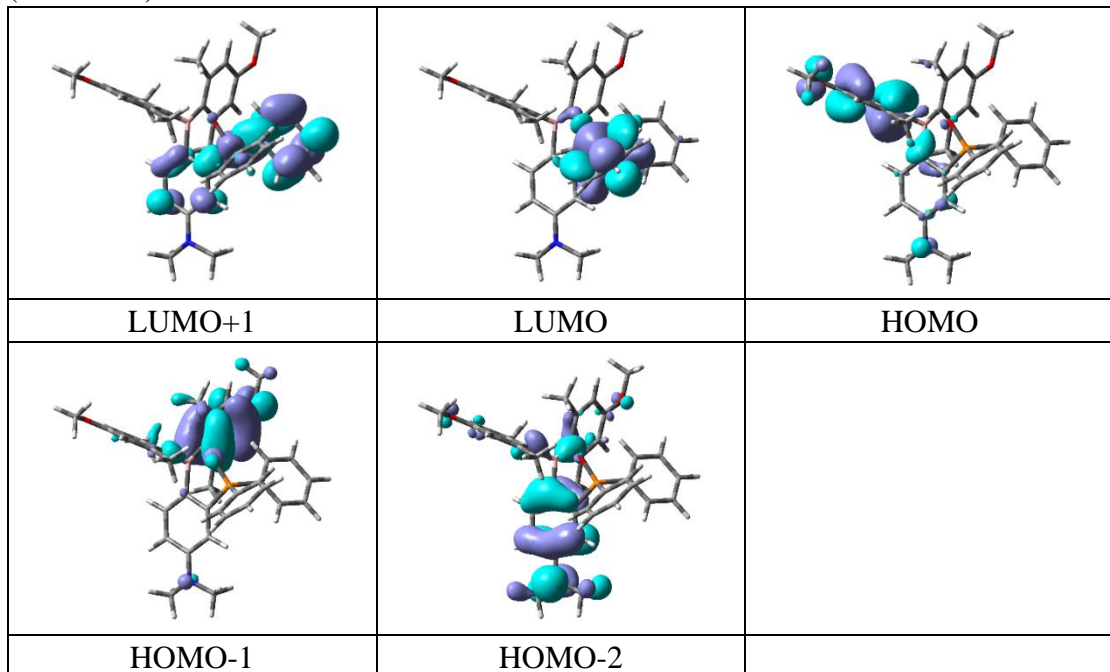


Table S7. TD-DFT calculated electronic transitions for **B4-closed** along with their corresponding excitation energies and oscillator strengths.

Compound	Spin State	Transition Configuration	Excitation Energy [nm (eV)]	Oscillator Strength
B4-closed	S1	HOMO-1→LUMO (6%)	379.93(3.26)	0.0054
		HOMO→LUMO (93%)		
	S2	HOMO-2→LUMO (3%)	360.80(3.44)	0.0040
		HOMO-1→LUMO (90%)		
		HOMO→LUMO (6%)		
	S3	HOMO-2→LUMO (81%)	345.14(3.59)	0.0144
		HOMO-1→LUMO (3%)		
		HOMO→LUMO+1 (14%)		
	S4	HOMO-2→LUMO (15%)	343.87(3.61)	0.0344
		HOMO→LUMO+1 (81%)		
	S5	HOMO-3→LUMO (99%)	335.23(3.70)	0.0004

Table S8. Primary orbitals which contribute to the calculated transitions of **B4-closed** (iso = 0.03).

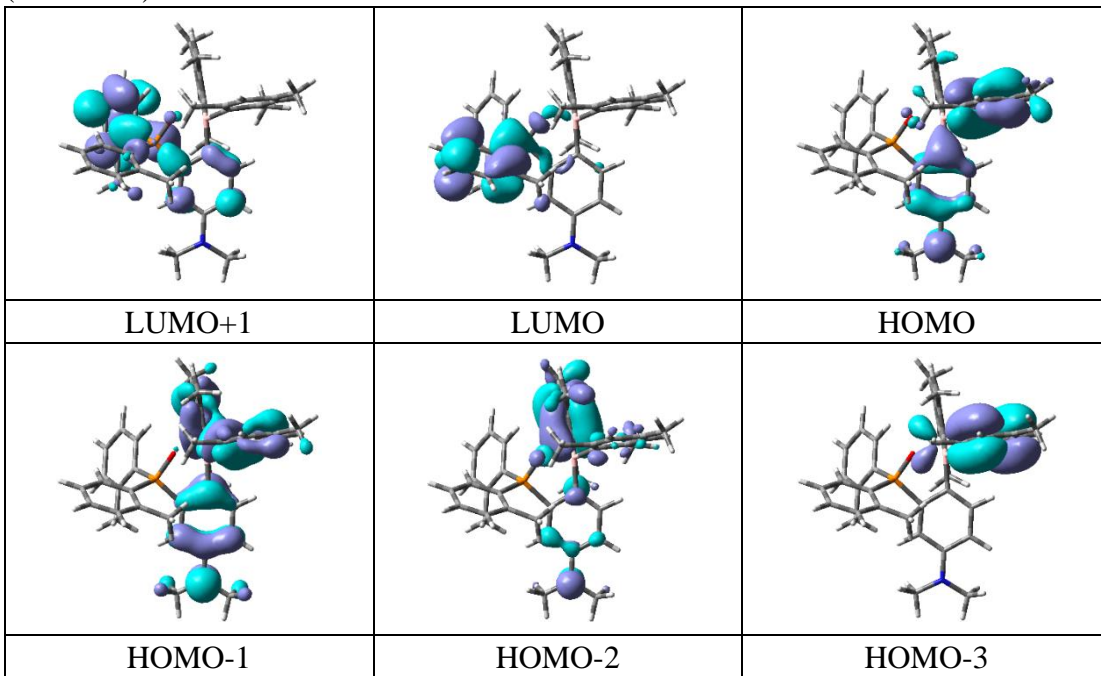


Table S9. TD-DFT calculated electronic transitions for **B2-open** along with their corresponding excitation energies and oscillator strengths.

Compound	Spin State	Transition Configuration	Excitation Energy [nm (eV)]	Oscillator Strength
B2-open	S1	HOMO-2→LUMO (6%)	324.60 (3.82)	0.3215
		HOMO-1→LUMO (10%)		
		HOMO→LUMO (76%)		
	S2	HOMO-3→LUMO (11%)	308.21 (4.02)	0.1265
		HOMO-2→LUMO (13%)		
		HOMO-1→LUMO (57%)		
		HOMO→LUMO (12%)		
	S3	HOMO-2→LUMO (72%)	290.87 (4.26)	0.0255
		HOMO-1→LUMO (19%)		
	S4	HOMO-3→LUMO (71%)	278.13 (4.46)	0.0078
		HOMO-1→LUMO (7%)		
		HOMO→LUMO (4%)		
		HOMO→LUMO+2 (8%)		
	S5	HOMO-4→LUMO (70%)	266.17 (4.66)	0.0183
		HOMO-4→LUMO+2 (2%)		
		HOMO-4→LUMO+5 (4%)		
		HOMO-3→LUMO+8 (3%)		
		HOMO→LUMO+2 (9%)		

Table S10. Primary orbitals which contribute to the calculated transitions of **B2-open** (iso = 0.03).

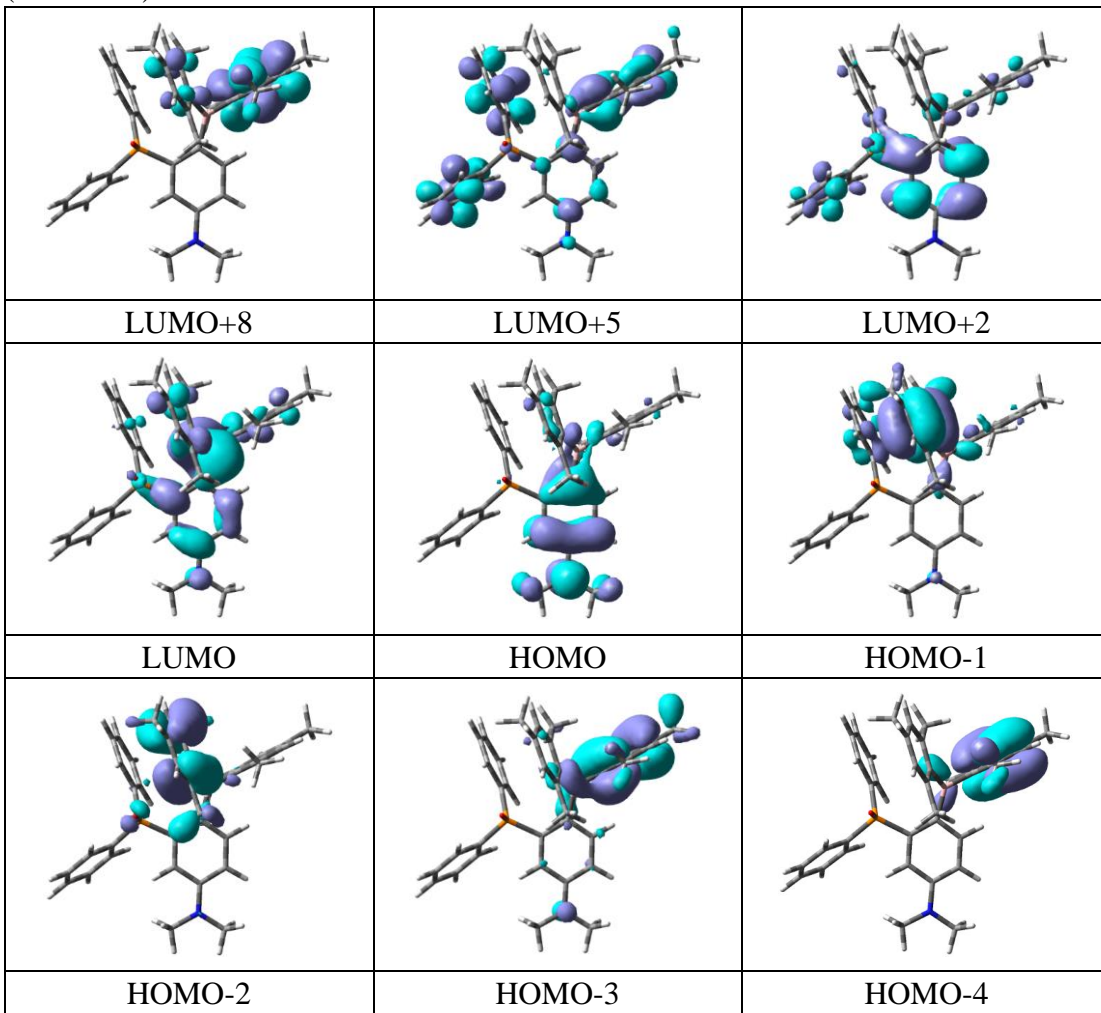
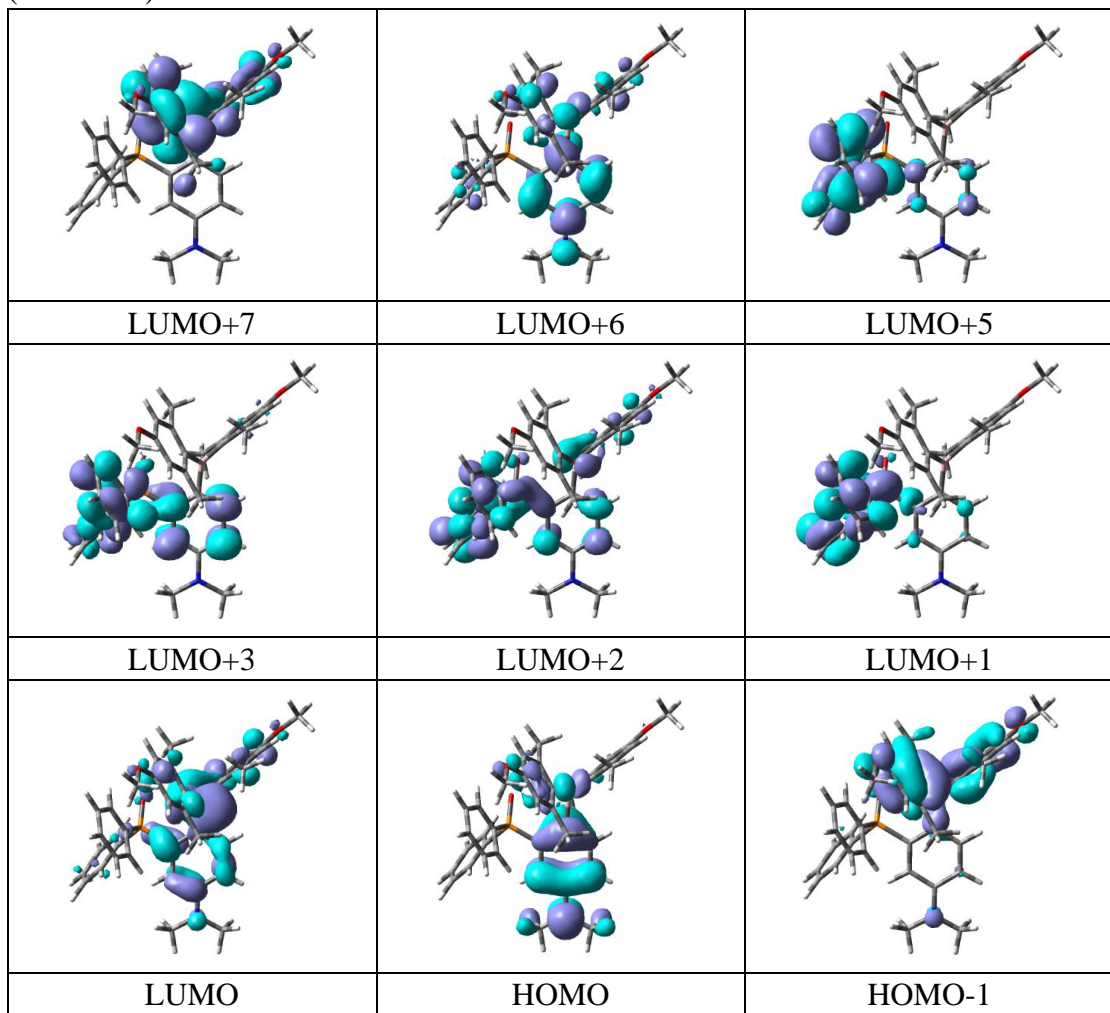


Table S11. TD-DFT calculated electronic transitions for **B3-open** along with their corresponding excitation energies and oscillator strengths.

Compound	Spin State	Transition Configuration	Excitation Energy [nm (eV)]	Oscillator Strength
B3-open	S1	HOMO-1→LUMO (49%)	313.33 (3.96)	0.1431
		HOMO-1→LUMO+2 (2%)		
		HOMO→LUMO (40%)		
	S2	HOMO-10→LUMO (2%)	305.16 (4.06)	0.2809
		HOMO-2→LUMO (6%)		
		HOMO-1→LUMO (38%)		
		HOMO→LUMO (45%)		
	S3	HOMO-2→LUMO (74%)	277.88 (4.46)	0.0017
		HOMO-1→LUMO (2%)		
		HOMO→LUMO (3%)		
		HOMO→LUMO+2 (4%)		

		HOMO→LUMO+3(5%)		
S4	HOMO-5→LUMO (3%)	263.52 (4.70)	0.0755	
	HOMO-3→LUMO (5%)			
	HOMO-2→LUMO (9%)			
	HOMO→LUMO+1 (11%)			
	HOMO→LUMO+2 (21%)			
	HOMO→LUMO+3 (23%)			
	HOMO→LUMO+5 (3%)			
	HOMO→LUMO+6 (3%)			
S5	HOMO-3→LUMO (70%)	261.86 (4.73)	0.0116	
	HOMO-3→LUMO+2 (3%)			
	HOMO-1→LUMO+7 (3%)			

Table S12. Primary orbitals which contribute to the calculated transitions of **B3-open** (iso = 0.03).



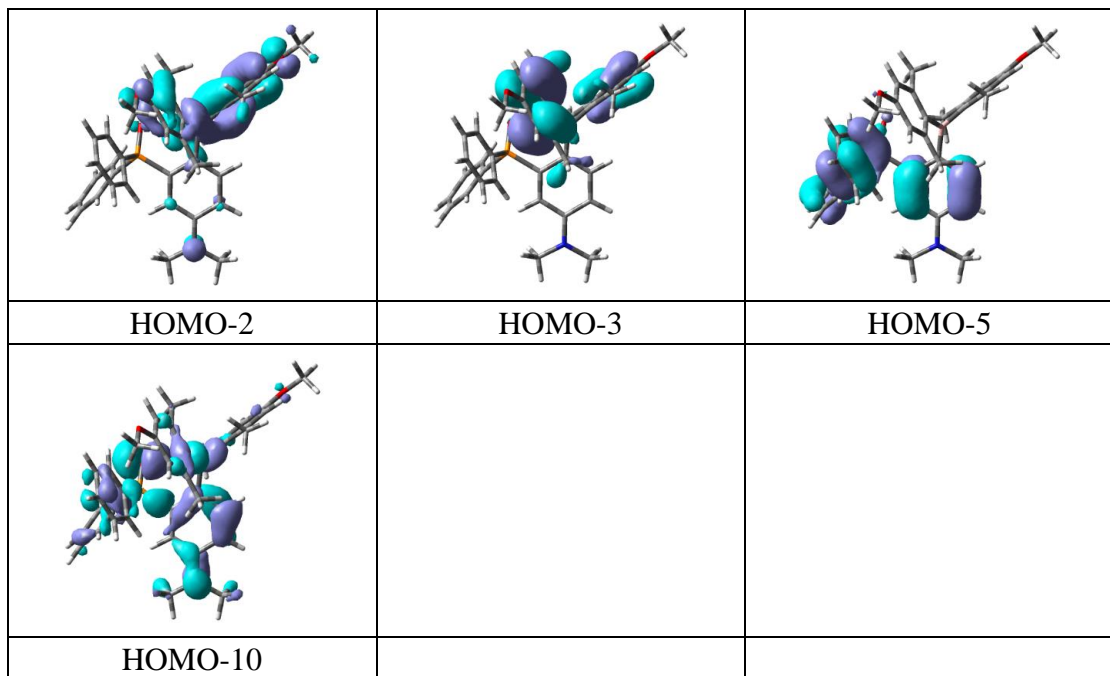


Table S13. TD-DFT calculated electronic transitions for **B4-open** along with their corresponding excitation energies and oscillator strengths.

Compound	Spin State	Transition Configuration	Excitation Energy [nm (eV)]	Oscillator Strength
B4-open	S1	HOMO-2→LUMO (2%)	327.24 (3.79)	0.2331
		HOMO-1→LUMO (23%)		
		HOMO→LUMO (68%)		
	S2	HOMO-3→LUMO (19%)	307.23 (4.04)	0.2086
		HOMO-2→LUMO (7%)		
		HOMO-1→LUMO (46%)		
		HOMO→LUMO (20%)		
	S3	HOMO-2→LUMO (76%)	290.90 (4.26)	0.0177
		HOMO-2→LUMO+7 (3%)		
		HOMO-1→LUMO(14%)		
	S4	HOMO-3→LUMO (68%)	280.07 (4.43)	0.0433
		HOMO-2→LUMO (6%)		
		HOMO-1→LUMO (9%)		
		HOMO→LUMO (5%)		
		HOMO→LUMO+3 (3%)		
	S5	HOMO-4→LUMO (83%)	267.15 (4.64)	0.0152
		HOMO-4→LUMO+3 (3%)		
		HOMO-4→LUMO+6 (4%)		
		HOMO-3→LUMO+8 (3%)		

Table S14. Primary orbitals which contribute to the calculated transitions of **B4-open** (iso = 0.03).

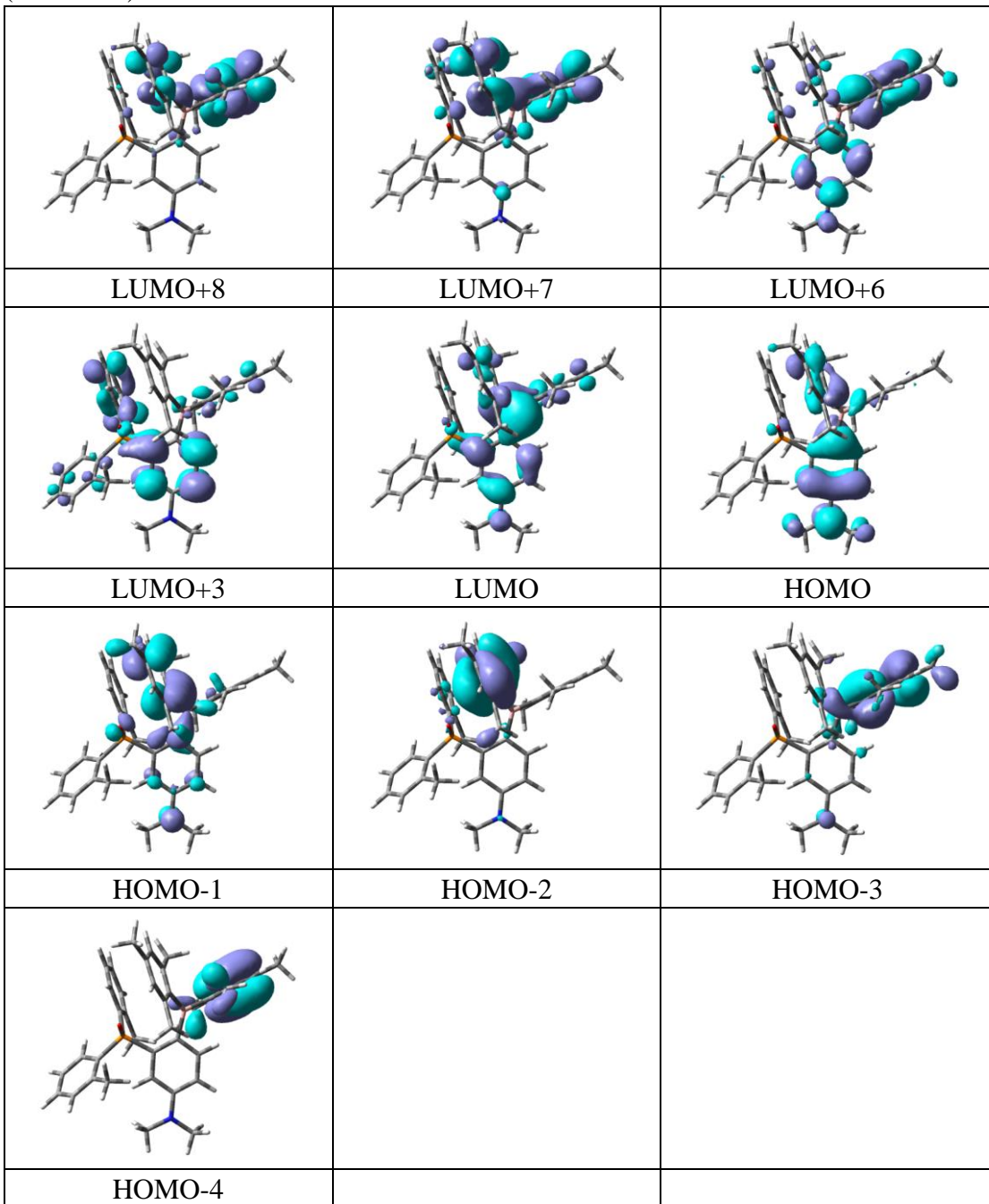


Table S15. Theoretical calculations of enthalpy for open and closed forms of **B2 (o-B2 and c-B2)** at different temperature

Temperature	o-B2 (enthalpy) HF	c-B2 (enthalpy) HF	Difference (close-open) HF	Difference of Enthalpy in kJ/mol
130 K	-1968.258719	-1968.266868	-0.008149	-21.40
200 K	-1968.248878	-1968.255962	-0.007084	-18.60
300 K	-1968.228639	-1968.233989	-0.00535	-14.05
340 K	-1968.218452	-1968.223057	-0.004605	-12.09

S3. NMR and HRMS Spectra

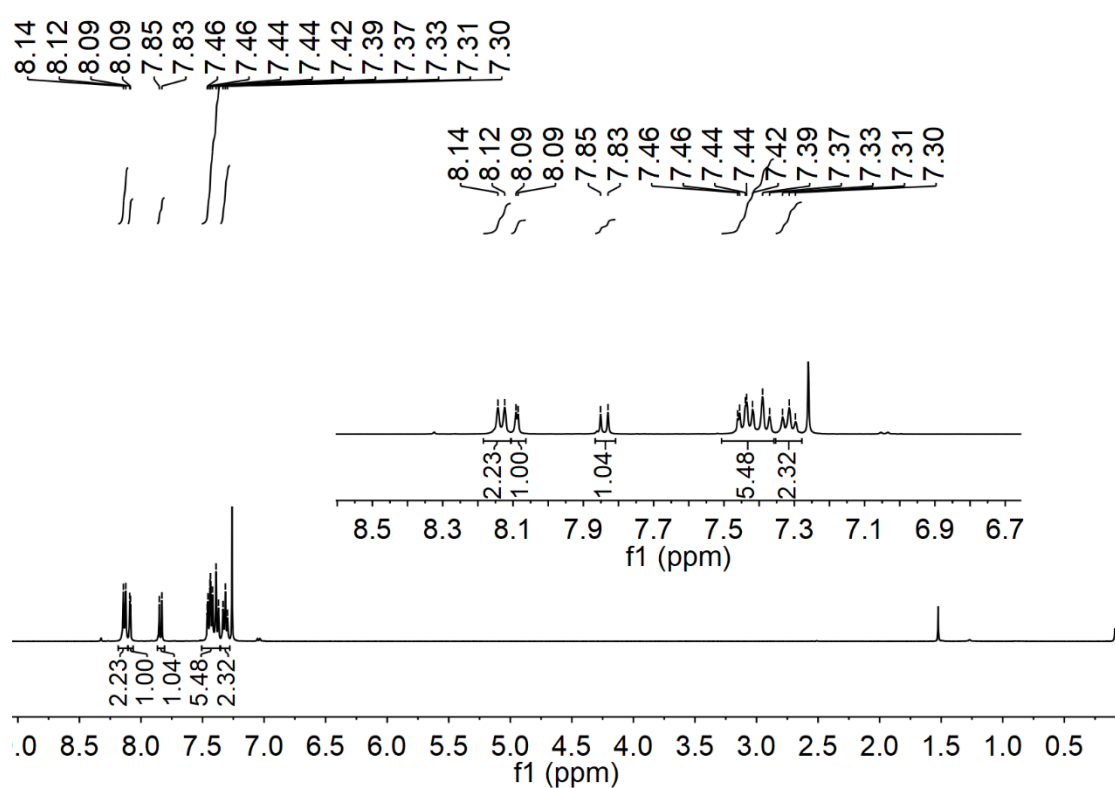


Figure S14. ¹H NMR (400 MHz, CDCl₃) spectrum of **B1-1**.

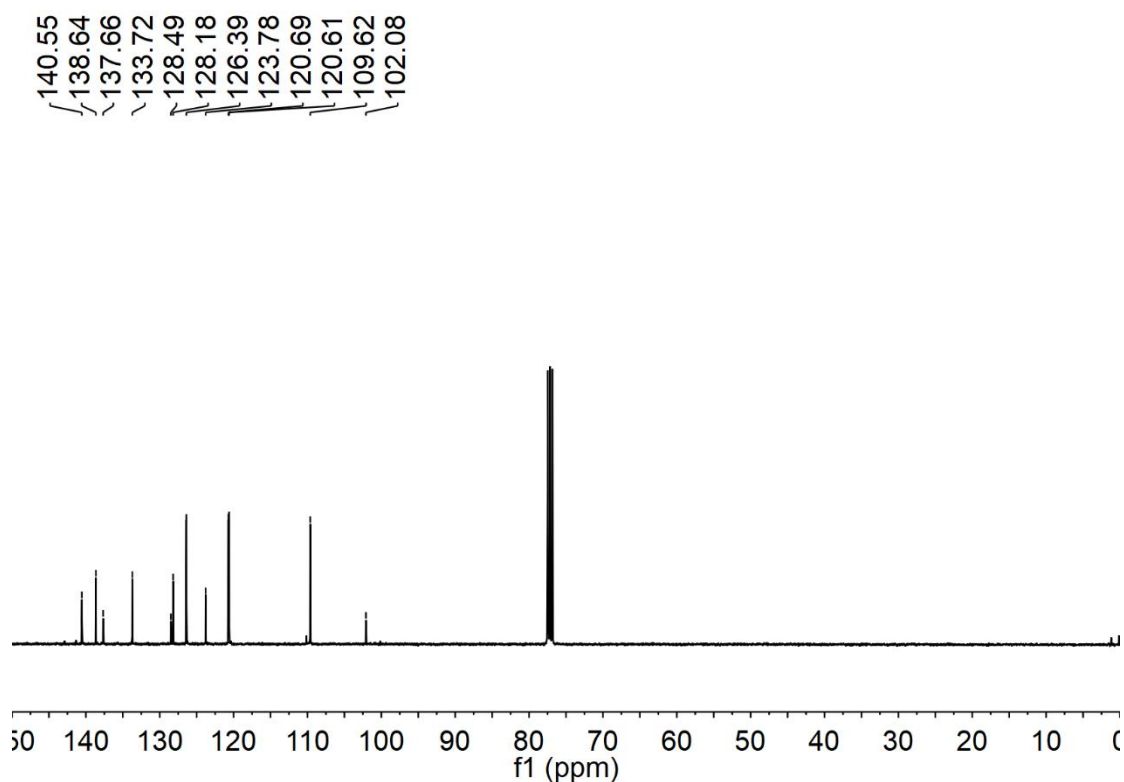


Figure S15. ¹³C NMR (101 MHz, CDCl₃) spectrum of **B1-1**.

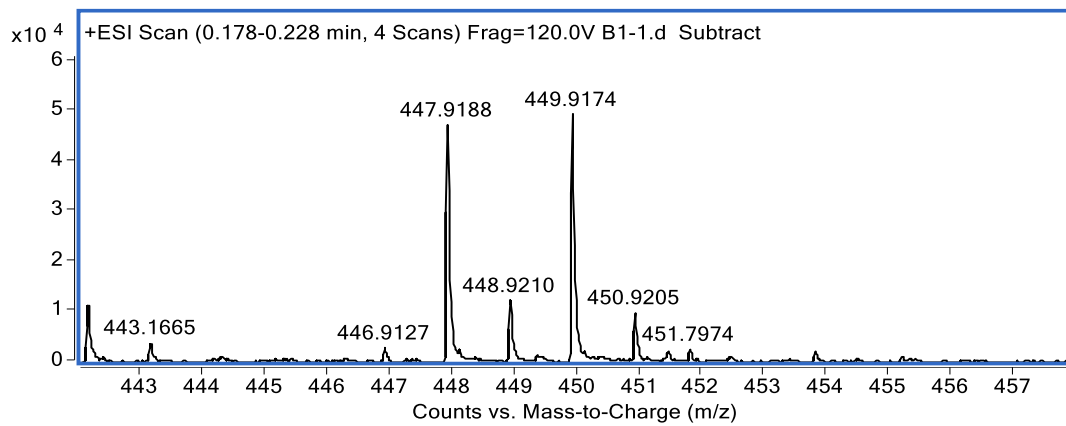
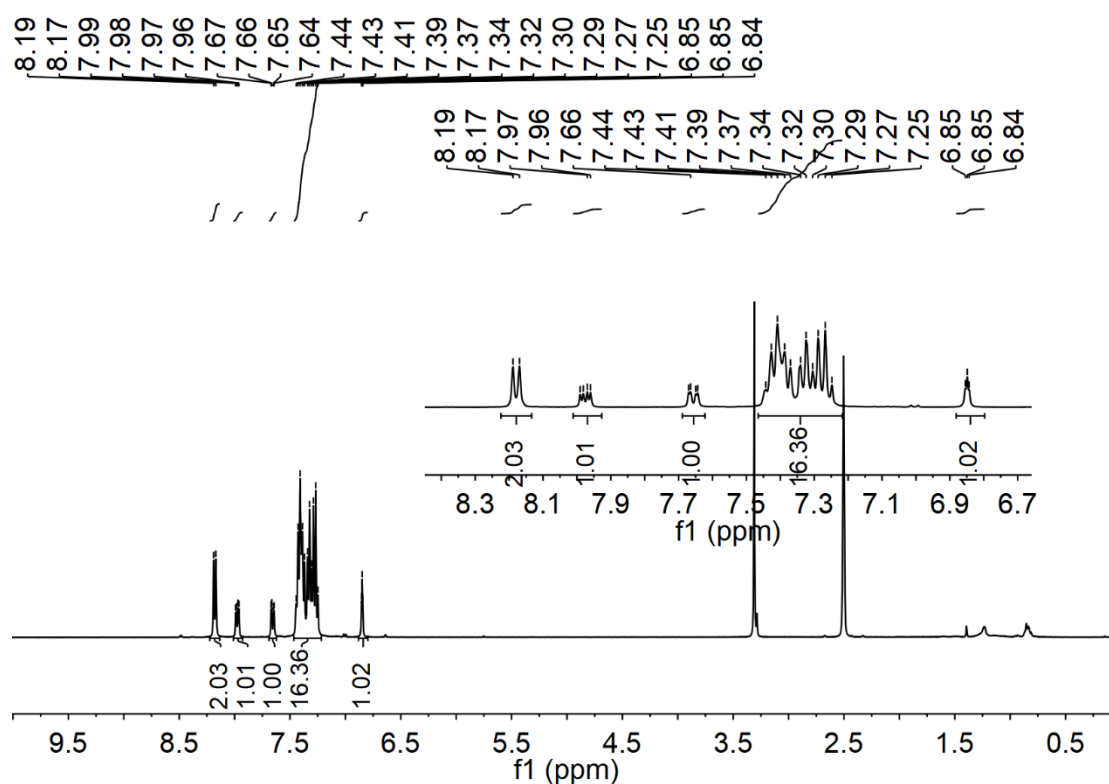


Figure S16. HRMS spectrum for **B1-1**.



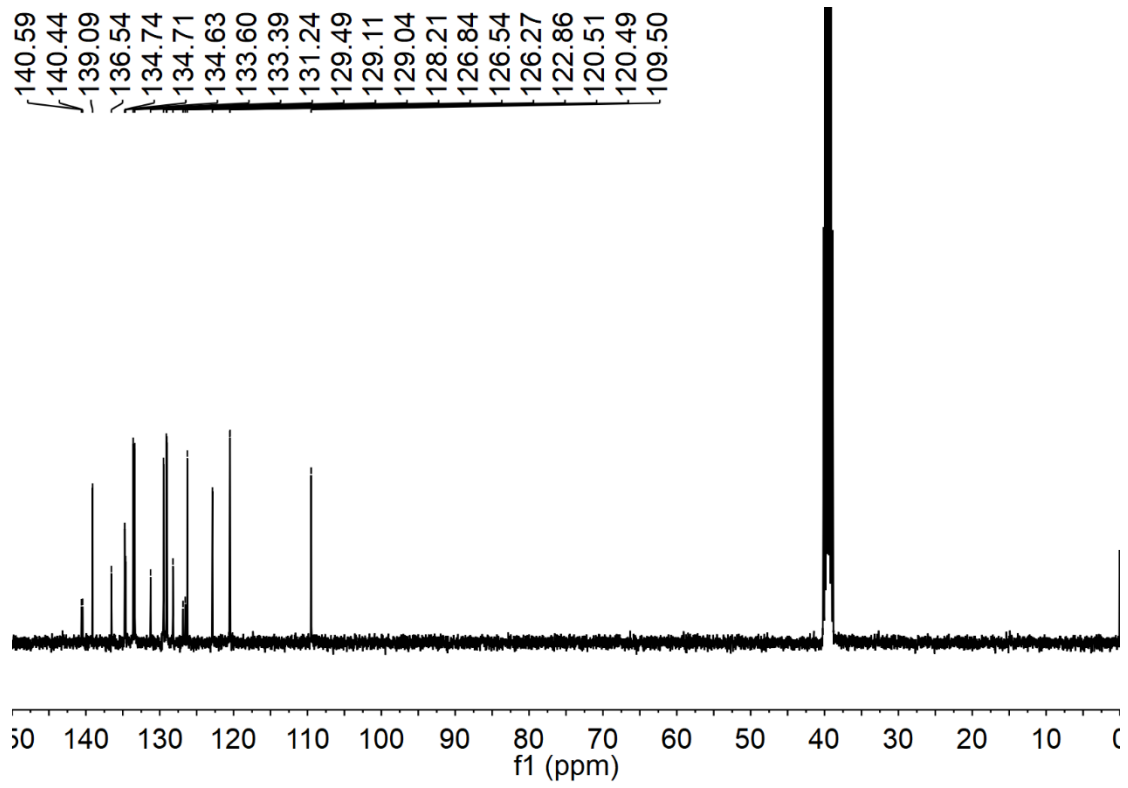


Figure S18. ¹³C NMR (101 MHz, DMSO-*d*₆) spectrum of **B1-2**.

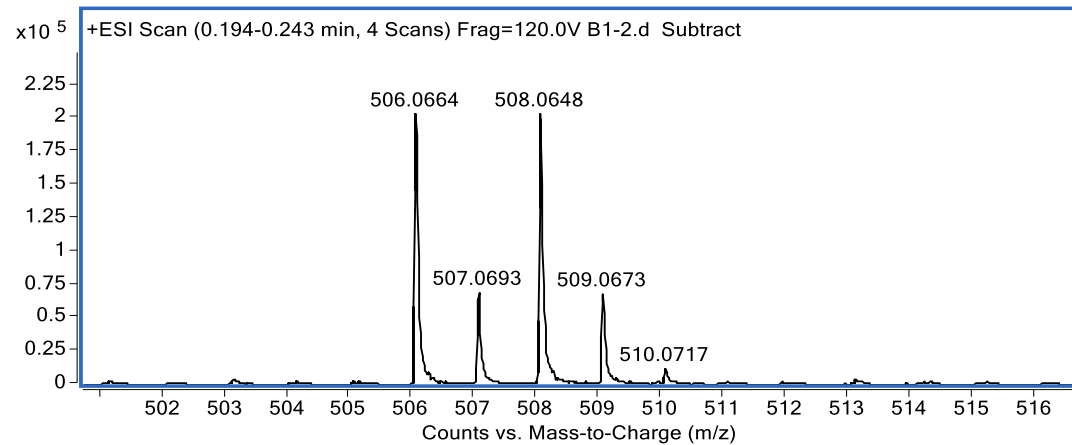


Figure S19. HRMS spectrum for **B1-2**.

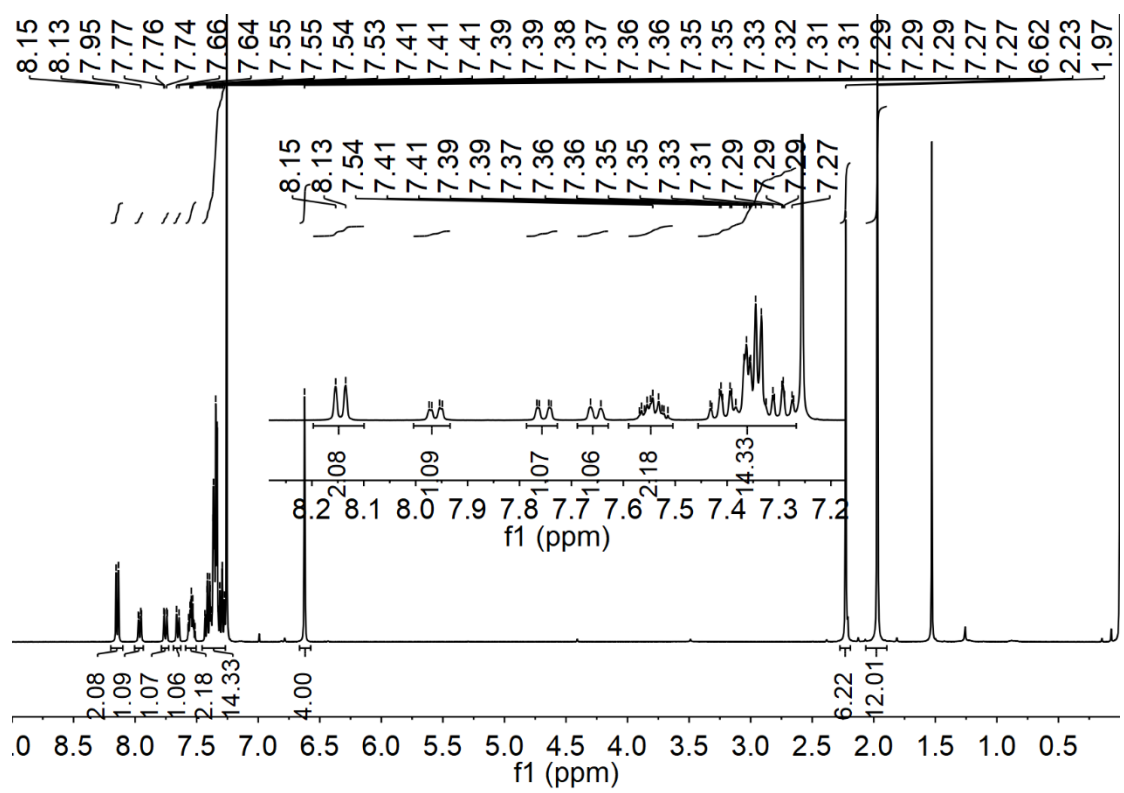


Figure S20. ^1H NMR (400 MHz, CDCl_3) spectrum of **B1**.

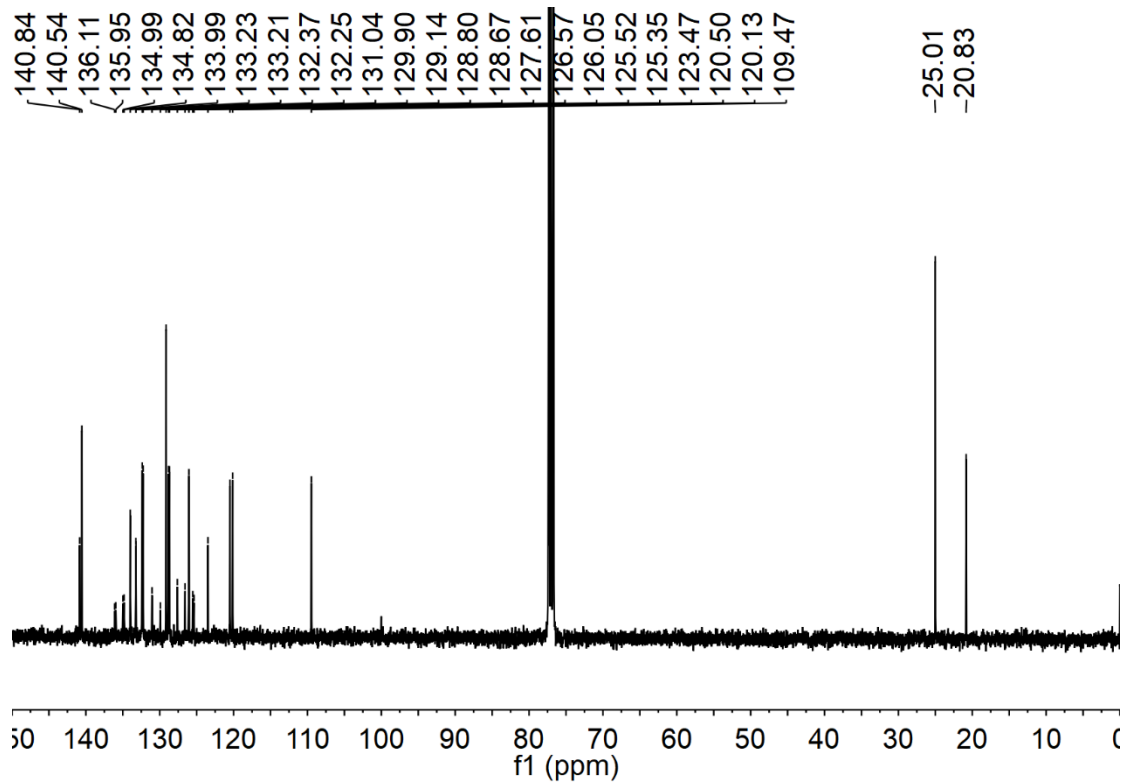


Figure S21. ^{13}C NMR (101 MHz, CDCl_3) spectrum of **B1**.

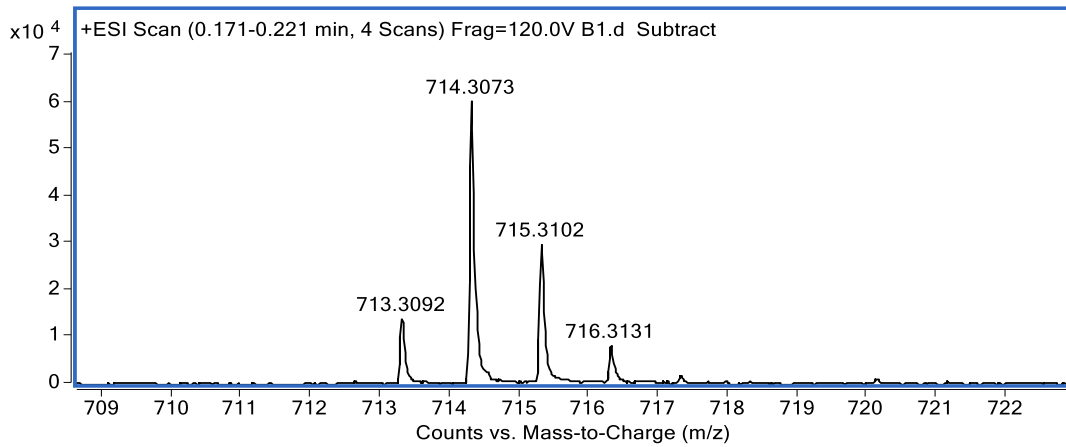


Figure S22. HRMS spectrum for **B1**.

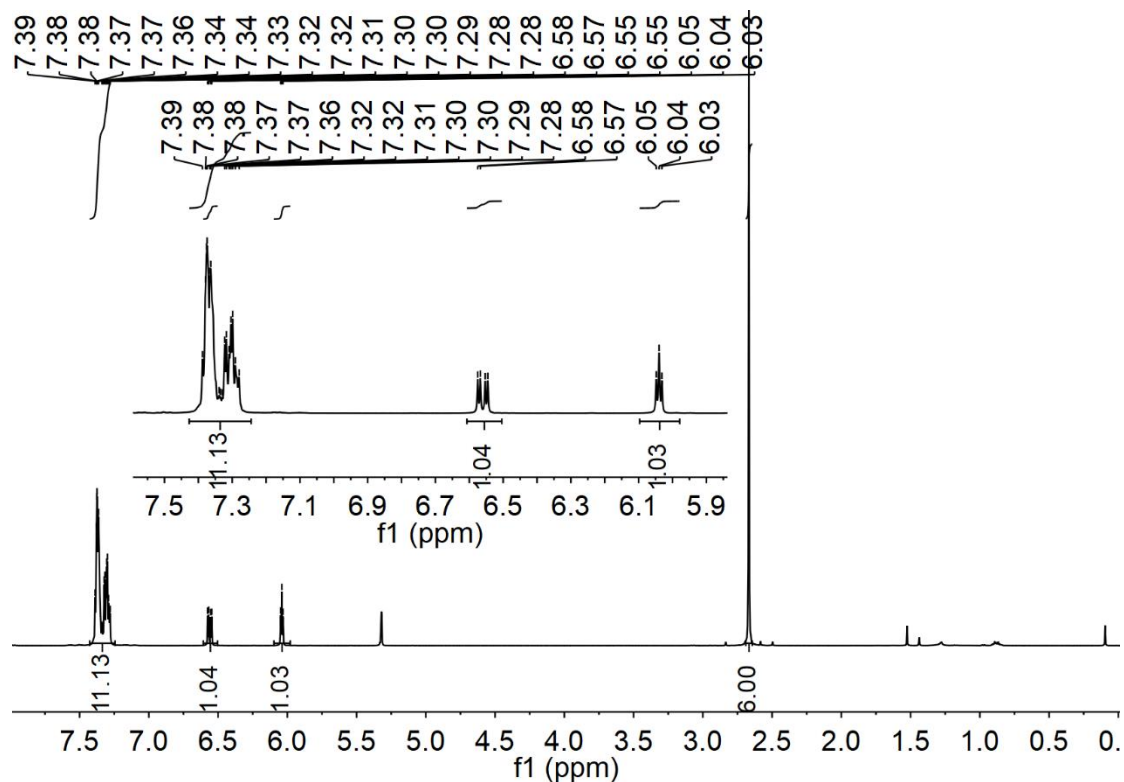


Figure S23. ^1H NMR (400 MHz, CD_2Cl_2) spectrum of **B2-1**.

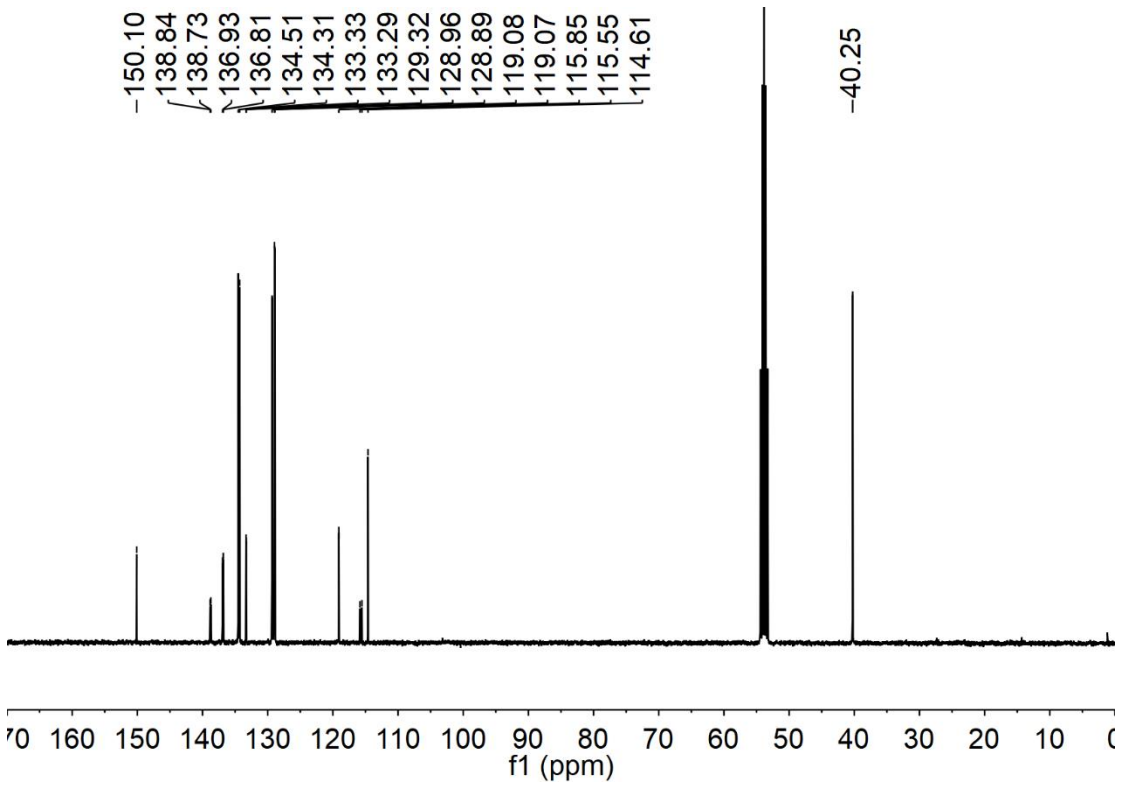


Figure S24. ¹³C NMR (101 MHz, CD₂Cl₂) spectrum of **B2-1**.

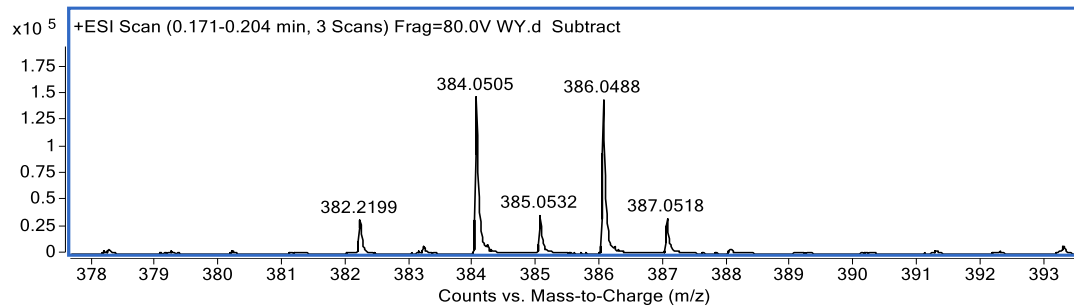


Figure S25. HRMS spectrum for **B2-1**.

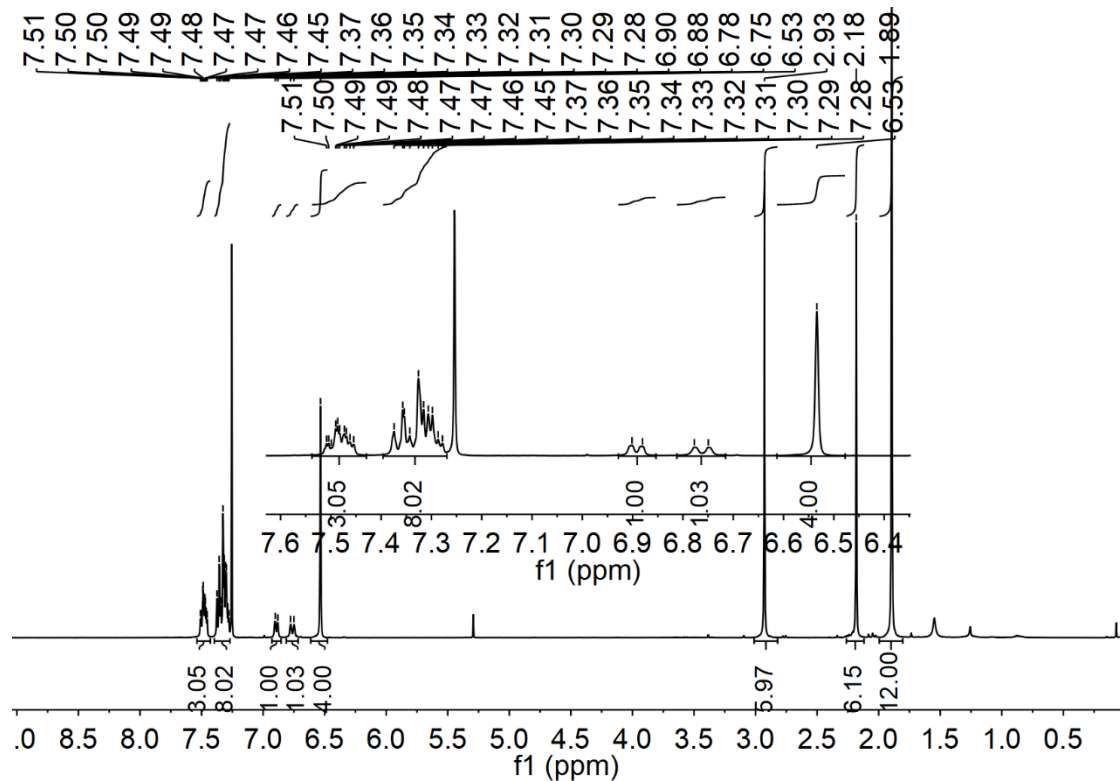


Figure S26. ^1H NMR (400 MHz, CDCl_3) spectrum of **B2**.

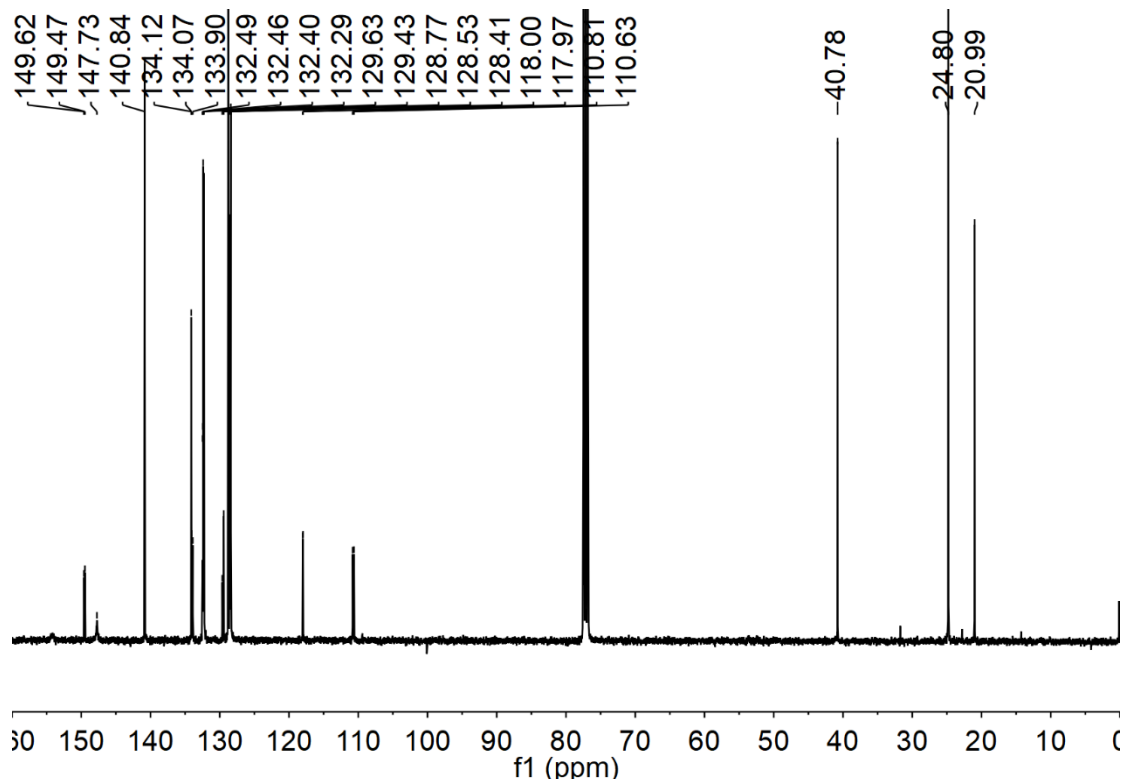


Figure S27. ^{13}C NMR (101 MHz, CDCl_3) spectrum of **B2**.

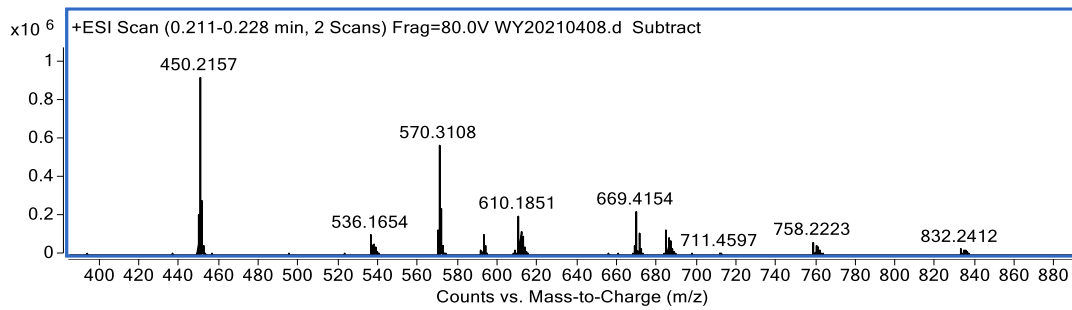


Figure S28. HRMS spectrum for **B2**.

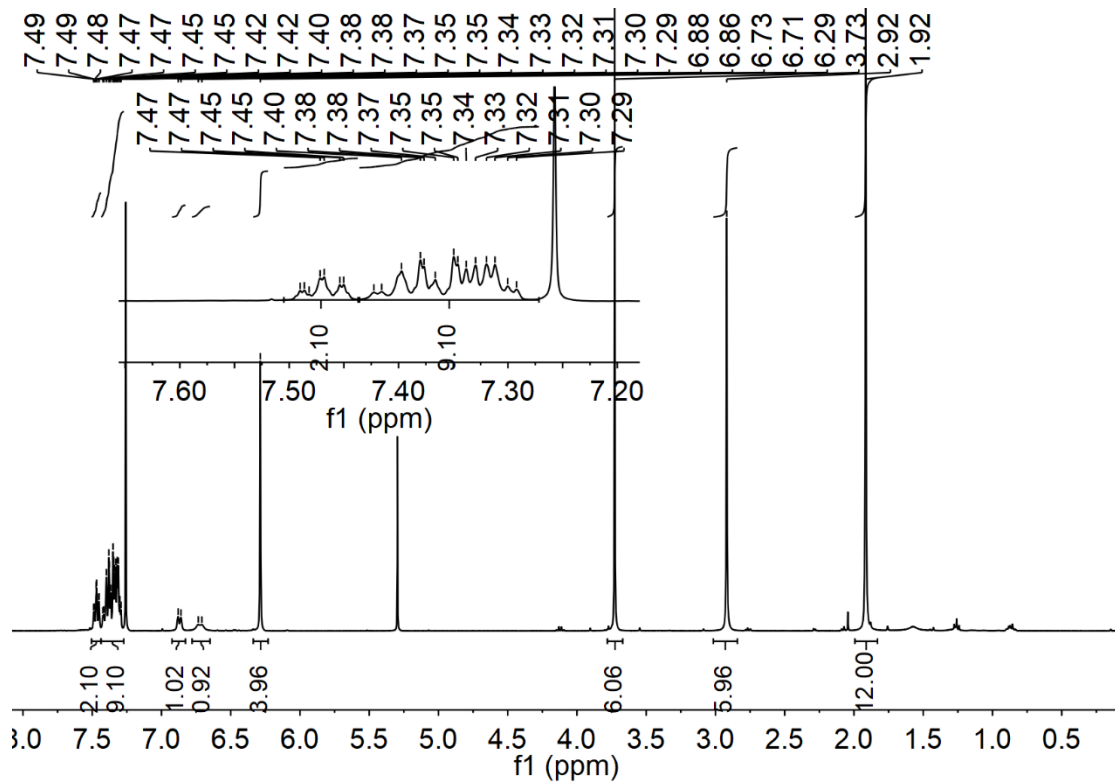


Figure S29. ^1H NMR (400 MHz, CDCl_3) spectrum of **B3**.

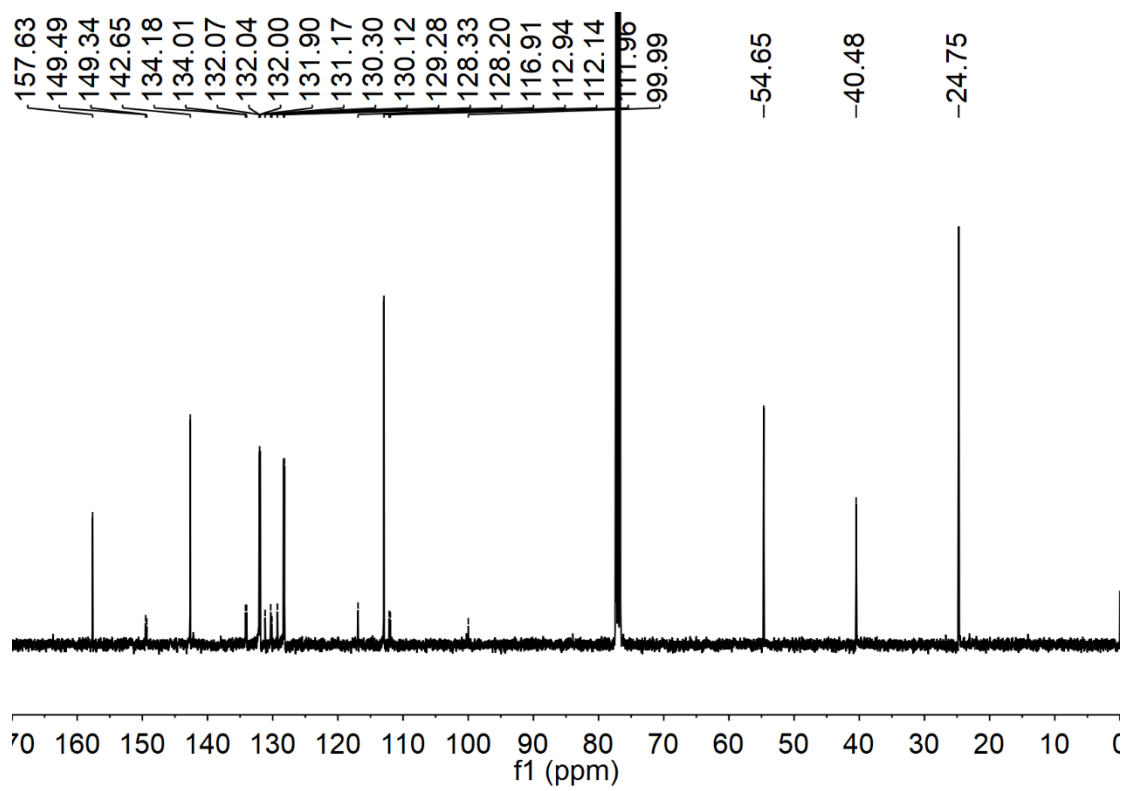


Figure S30. ¹³C NMR (101 MHz, CDCl₃) spectrum of **B3**.

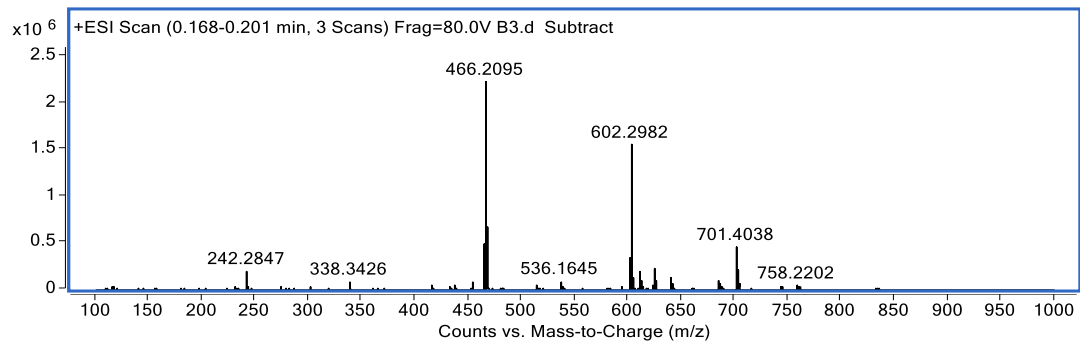


Figure S31. HRMS spectrum for **B3**.

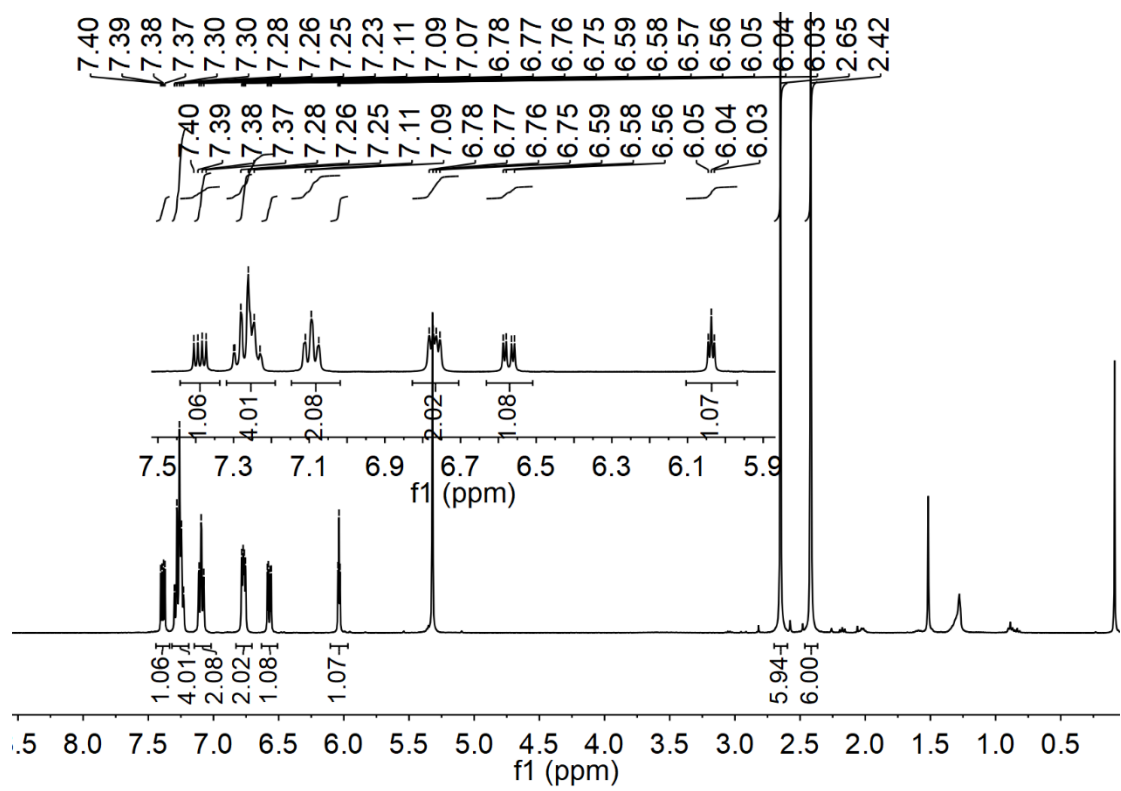


Figure S32. ^1H NMR (400 MHz, CD_2Cl_2) spectrum of **B4-1**.

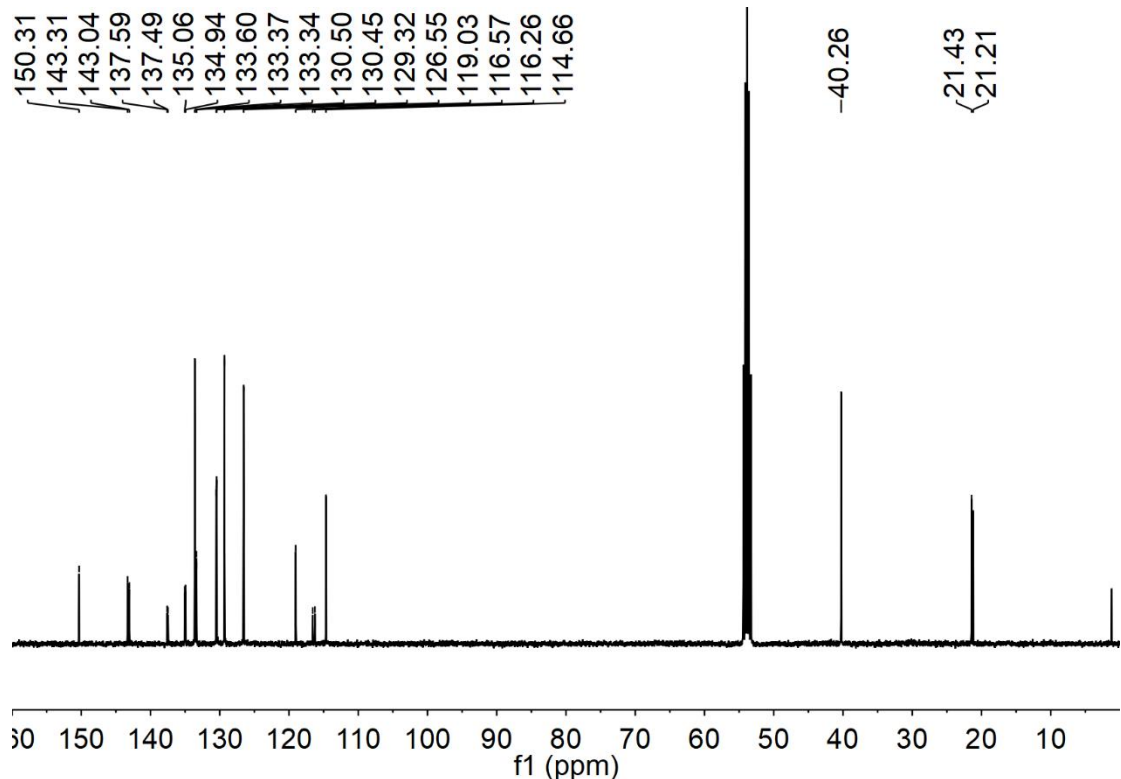


Figure S33. ^{13}C NMR (101 MHz, CD_2Cl_2) spectrum of **B4-1**.

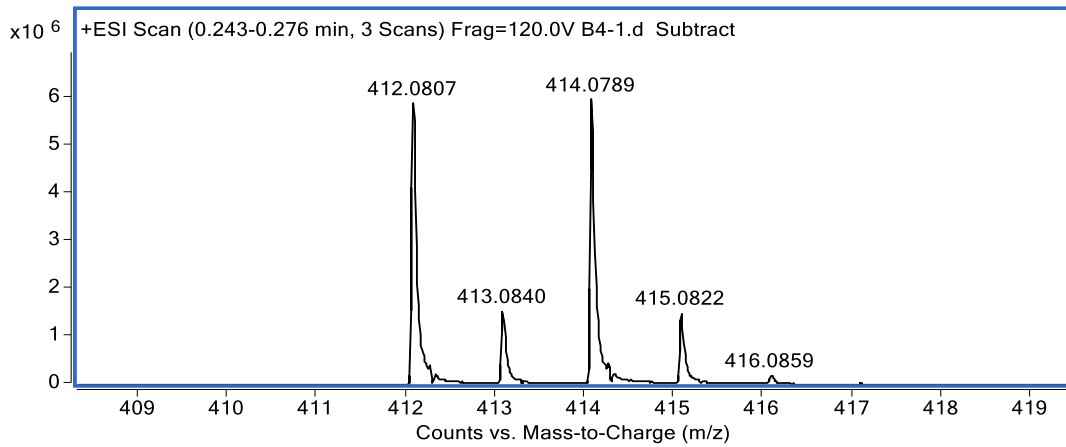


Figure 34. HRMS spectrum for **B4-1**.

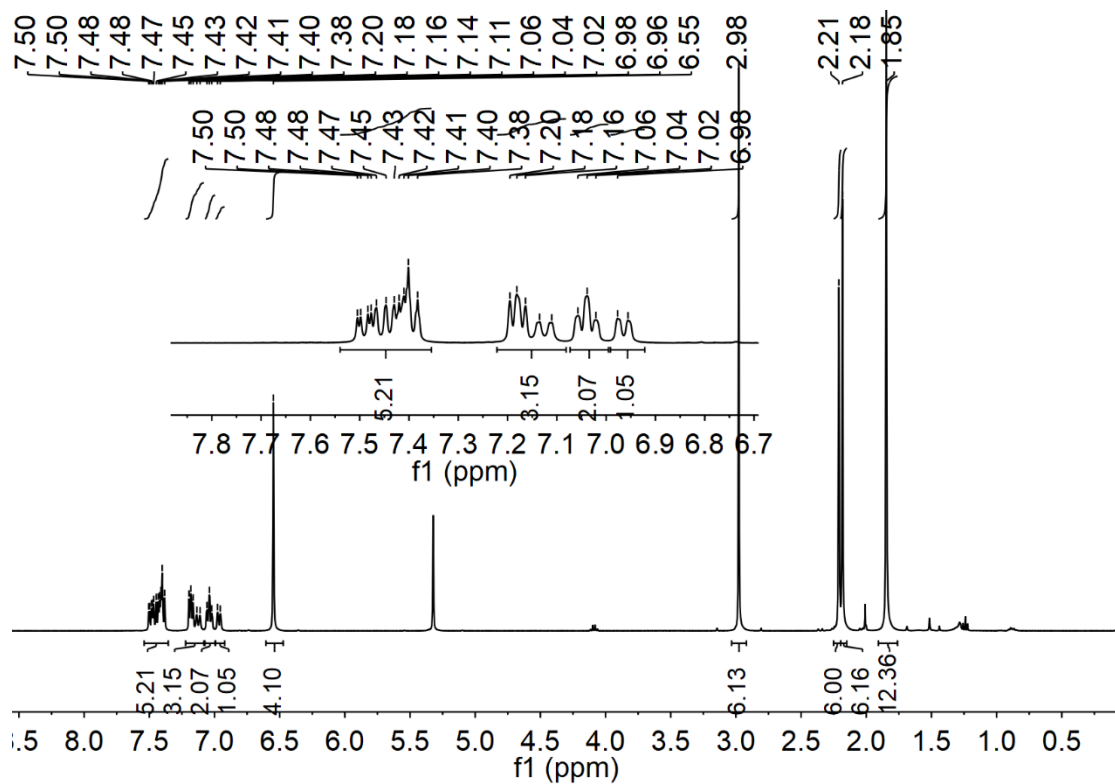


Figure S35. ¹H NMR (400 MHz, CD₂Cl₂) spectrum of **B4**.

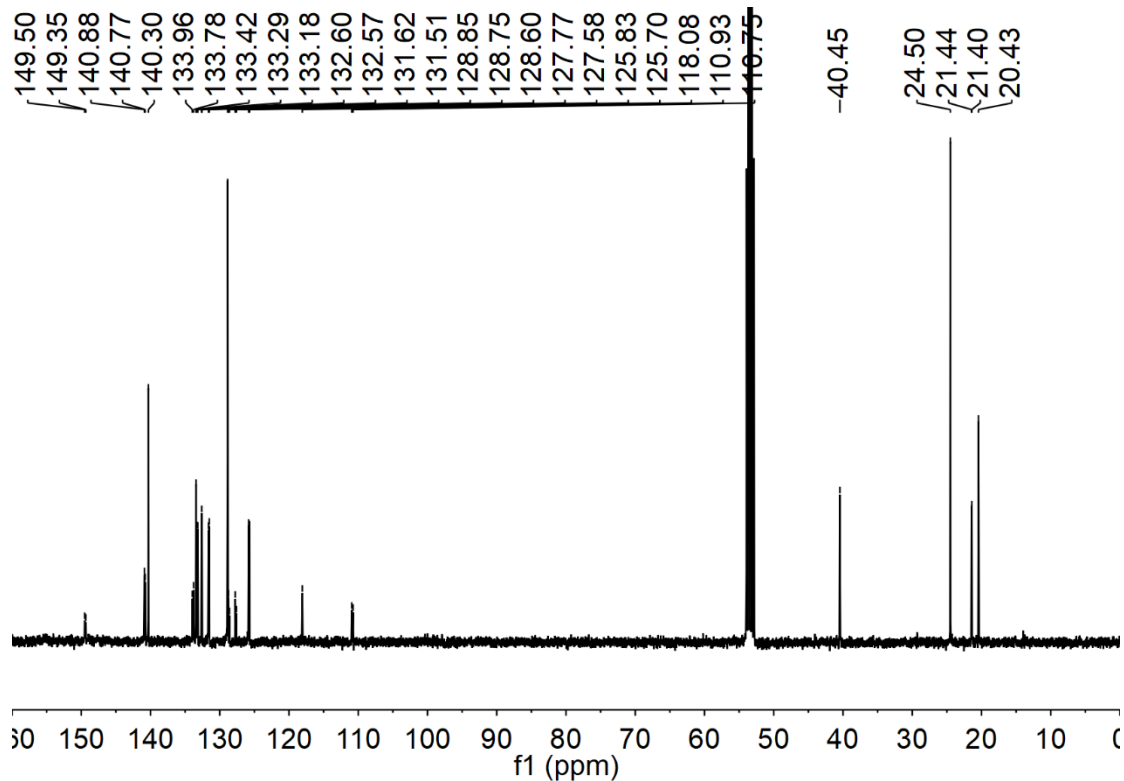


Figure S36. ^{13}C NMR (101 MHz, CD_2Cl_2) spectrum of **B4**.

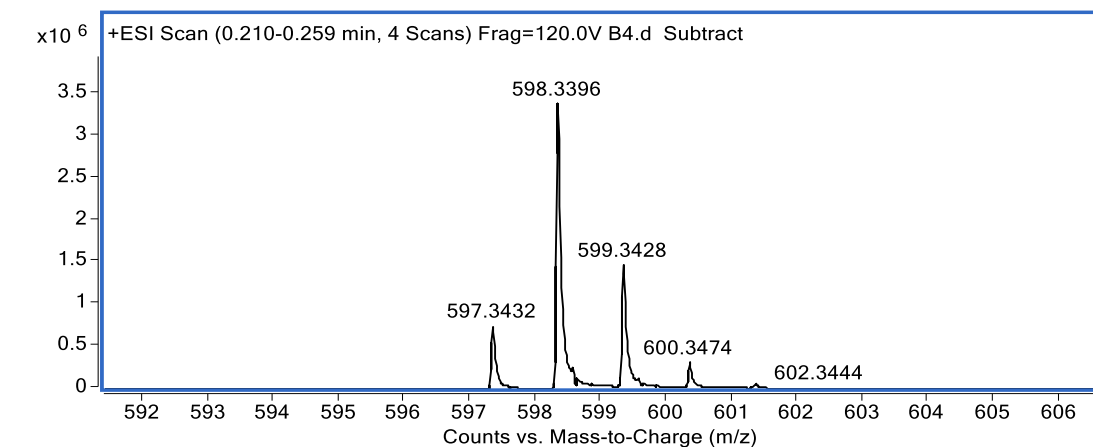


Figure S37. HRMS spectrum for **B4**.

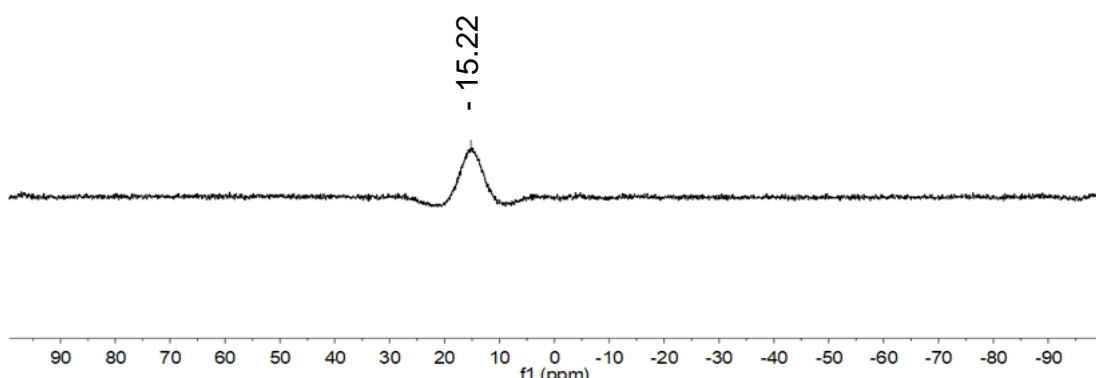


Figure S38. ^{11}B NMR (128 MHz, CDCl_3) spectrum of **B1**.

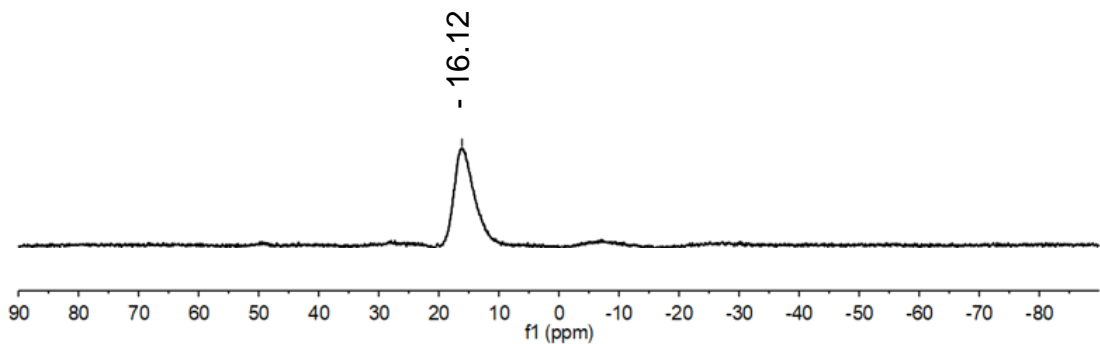


Figure S39. ¹¹B NMR (128 MHz, Acetone-*d*₆) spectrum of **B3**.

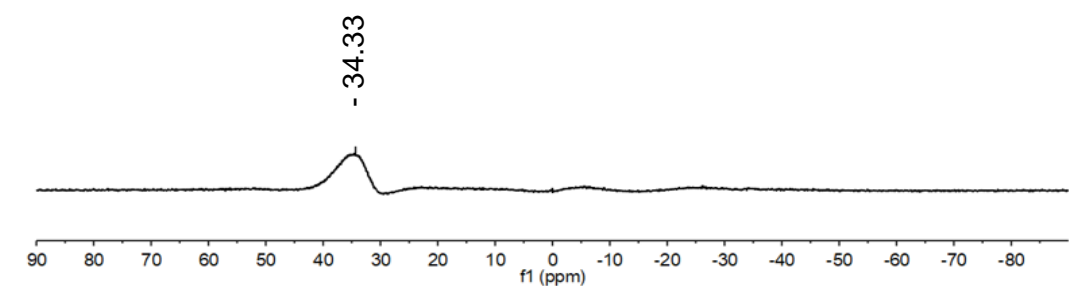


Figure S40. ¹¹B NMR (128 MHz, CDCl₃) spectrum of **B3**.

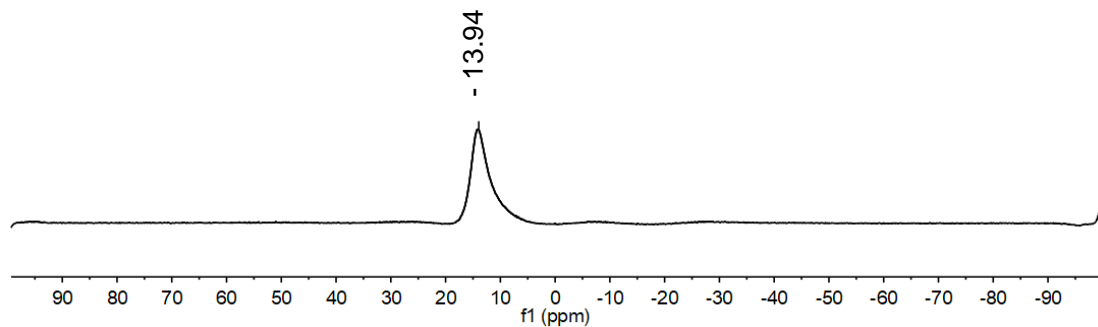


Figure S41. ¹¹B NMR (128 MHz, Acetone-*d*₆) spectrum of **B4**.

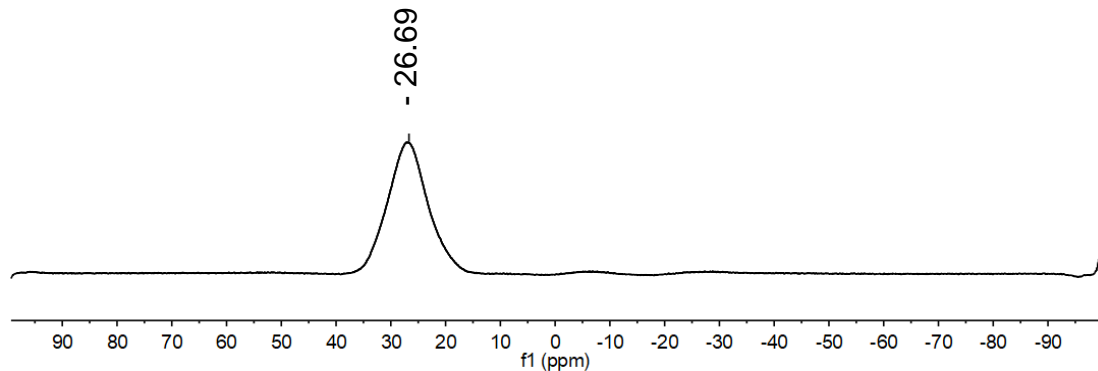


Figure S42. ¹¹B NMR (128 MHz, CDCl₃) spectrum of **B4**.

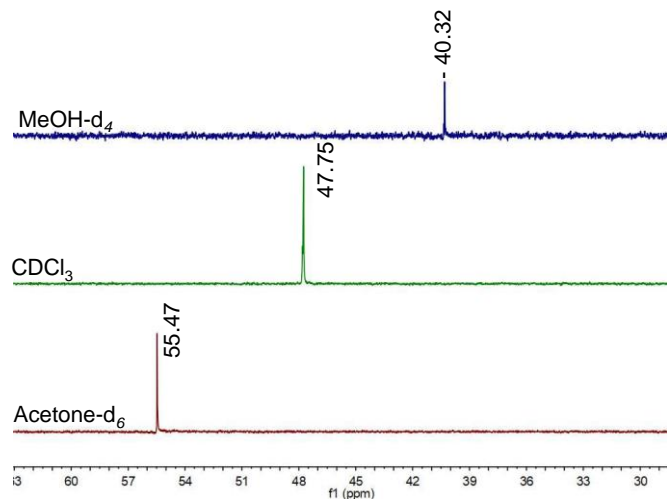


Figure S43. ^{31}P NMR spectra of **B3** in various solvents.

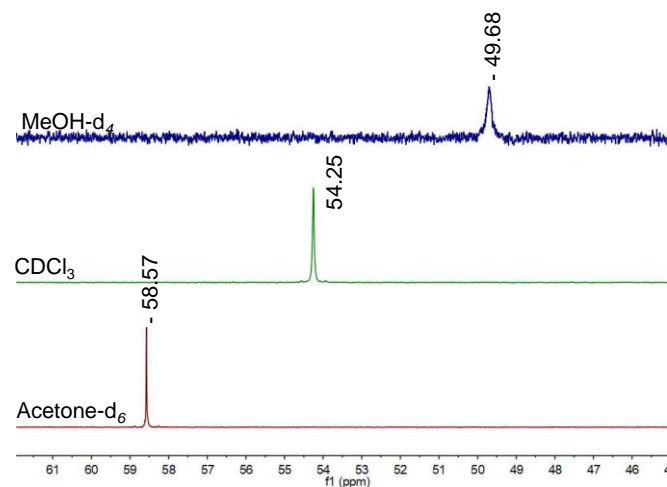


Figure S44. ^{31}P NMR spectra of **B4** in various solvents.

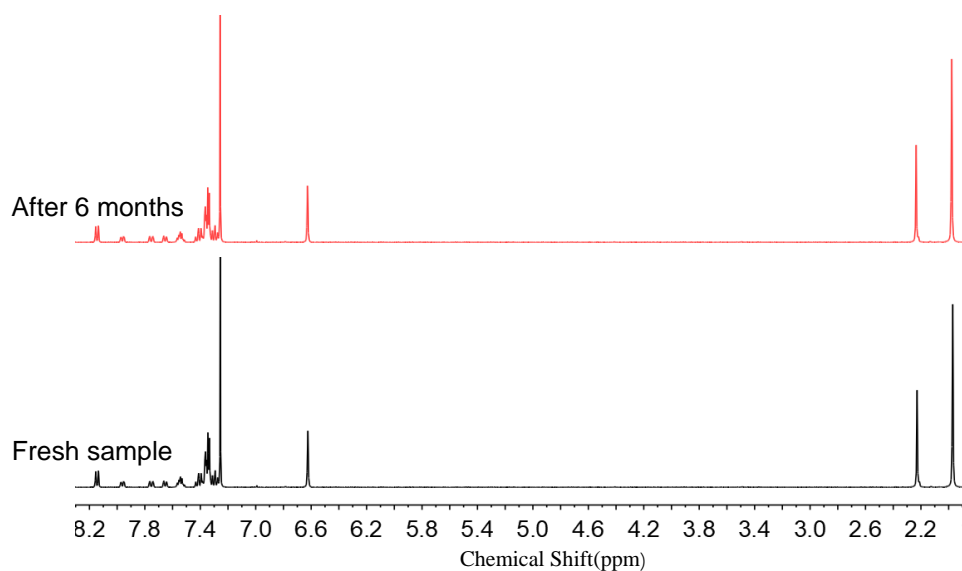


Figure S45. ^1H NMR (400 MHz, CDCl_3) spectra of **B1** at fresh state (black) and after 6 months (red).

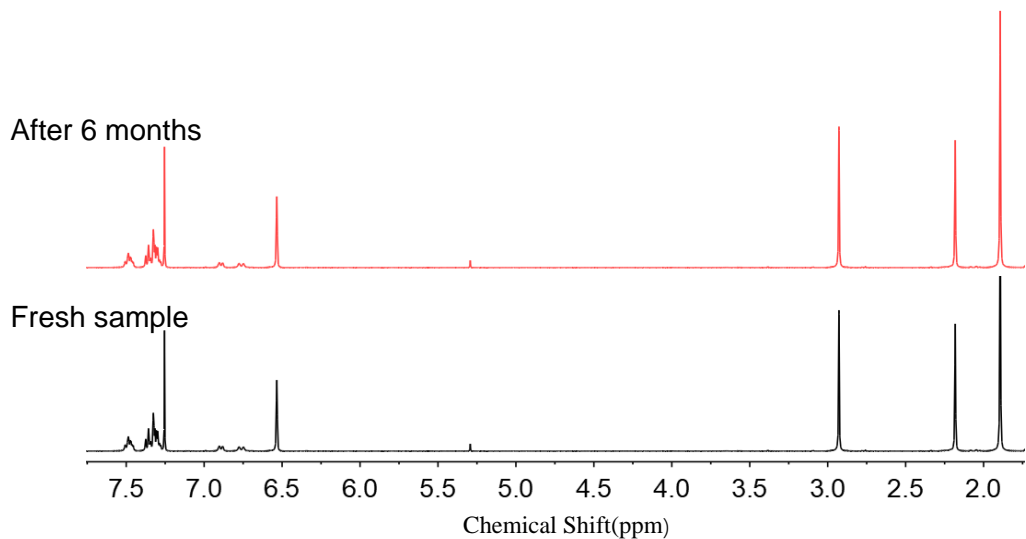


Figure S46. ^1H NMR (400 MHz, CDCl_3) spectra of **B2** at fresh state (black) and after 6 months (red).

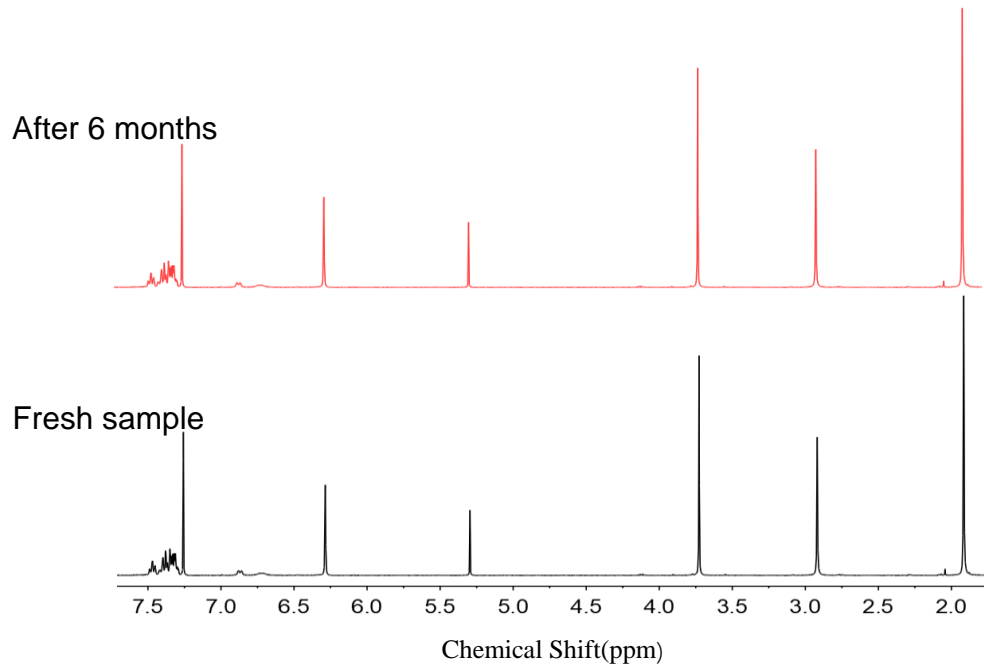


Figure S47. ^1H NMR (400 MHz, CDCl_3) spectra of **B3** at fresh state (black) and after 6 months (red).

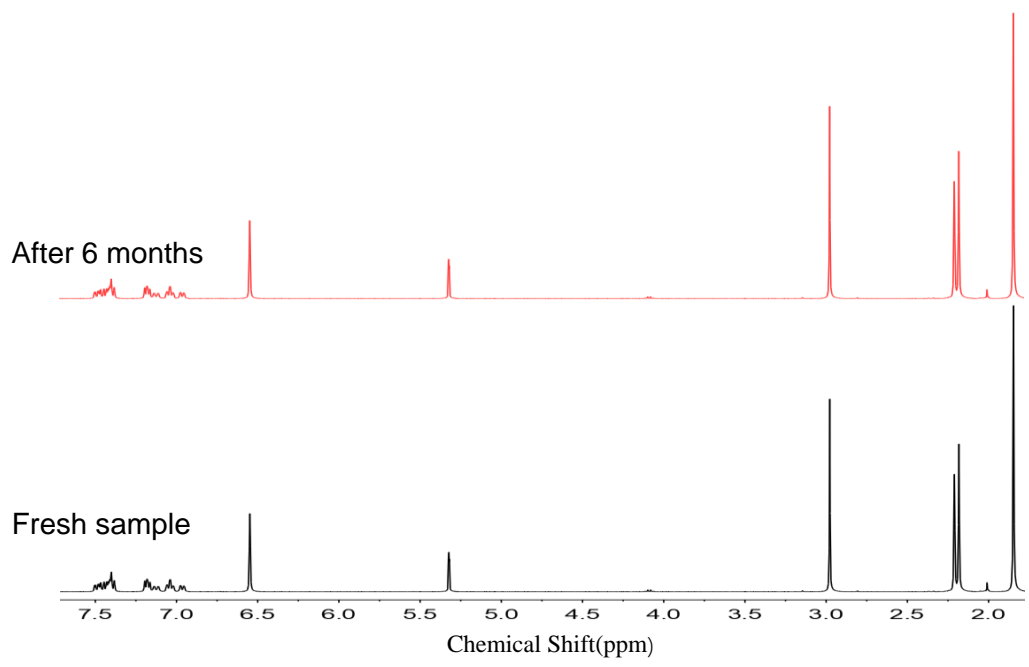


Figure S48. ¹H NMR (400 MHz, CD₂Cl₂) spectra of **B4** at fresh state (black) and after 6 months (red).

S4. X-ray Crystallographic Data

Table S16. Crystal data and structure refinement for **B2**.

Identification code	B2
Empirical formula	C ₃₈ H ₄₂ BNOP
Formula weight	569.54
Temperature/K	180.0
Crystal system	monoclinic
Space group	C2
a/Å	10.9945(6)
b/Å	21.3830(11)
c/Å	14.8510(7)
α/°	90
β/°	99.375(2)
γ/°	90
Volume/Å ³	3444.8(3)
Z	4
ρ _{calc} g/cm ³	1.1676
μ/mm ⁻¹	0.113
F(000)	1296.9
Crystal size/mm ³	0.47 × 0.32 × 0.3
Radiation	MoKα ($\lambda = 0.71073$)
2Θ range for data collection/°	4.22 to 55.12
Index ranges	-14 ≤ h ≤ 14, -27 ≤ k ≤ 27, -17 ≤ l ≤ 19
Reflections collected	24348
Independent reflections	7902 [R _{int} = 0.0255, R _{sigma} = 0.0320]
Data/restraints/parameters	7902/1/397
Goodness-of-fit on F ²	1.029
Final R indexes [I>=2σ (I)]	R ₁ = 0.0377, wR ₂ = 0.0968
Final R indexes [all data]	R ₁ = 0.0426, wR ₂ = 0.0997
Largest diff. peak/hole / e Å ⁻³	0.25/-0.28

Table S17. Fractional Atomic Coordinates ($\times 10^4$) and Equivalent Isotropic Displacement Parameters (Å² $\times 10^3$) for **B2**. Ueq is defined as 1/3 of the trace of the orthogonalised U_{ij} tensor.

Atom	x	y	z	U(eq)
B1	2838.3(15)	5484.9(8)	2745.9(11)	23.7(3)
C1	8025.1(18)	3739.8(11)	3456.2(16)	54.0(5)
C2	6569(2)	3037.1(11)	2491(2)	62.4(6)

C3	5881.4(14)	4062.3(8)	2935.1(11)	29.1(3)
C4	6042.1(14)	4600.4(7)	3486.3(11)	30.2(3)
C5	5137.2(14)	5047.5(7)	3468.6(11)	28.3(3)
C6	3997.4(13)	5000.2(7)	2884.5(10)	23.4(3)
C7	3837.3(12)	4444.4(8)	2377.6(9)	24.4(3)
C8	4735.8(14)	3982.6(7)	2379.3(11)	27.7(3)
C9	2532.6(13)	5680.0(7)	3750.2(10)	24.7(3)
C10	1827.3(14)	5306.5(7)	4263.6(10)	27.0(3)
C11	1639.1(15)	5497.1(8)	5127.2(11)	30.5(3)
C12	2142.2(15)	6038.2(8)	5538.9(11)	31.9(3)
C13	2859.7(15)	6394.9(8)	5055.1(11)	31.2(3)
C14	3062.9(14)	6224.8(7)	4182.7(10)	26.8(3)
C15	1274.5(19)	4686.3(9)	3935.3(13)	41.4(4)
C16	1929(2)	6211.1(10)	6482.9(13)	46.7(5)
C17	3870.7(15)	6662.4(8)	3737.4(11)	32.8(3)
C18	2785.5(14)	6038.4(7)	1969.2(10)	24.4(3)
C19	3683.8(15)	6143.2(8)	1402.6(11)	29.9(3)
C20	3447.3(16)	6557.1(8)	662.5(12)	33.4(4)
C21	2353.0(16)	6877.6(8)	444.8(11)	34.5(4)
C22	1481.5(15)	6788.0(8)	1005.8(11)	31.0(3)
C23	1673.5(14)	6385.4(7)	1752.8(10)	26.4(3)
C24	651.3(15)	6335.5(8)	2314.8(11)	31.6(3)
C25	2116(2)	7307.1(11)	-378.9(14)	49.8(5)
C26	4937.0(17)	5838.8(9)	1540.2(15)	43.5(4)
C27	1481.2(14)	3762.0(7)	1850.7(10)	25.9(3)
C28	355.6(17)	3670.6(8)	1281.8(12)	38.5(4)
C29	-314.9(19)	3132.7(10)	1370.5(14)	48.1(5)
C30	109(2)	2692.9(9)	2025.1(14)	43.5(4)
C31	1205(2)	2782.3(9)	2593.1(14)	45.2(5)
C32	1902.7(17)	3318.3(8)	2511.8(12)	36.9(4)
C33	2290.7(14)	4618.6(7)	566.4(10)	27.5(3)
C34	1669(2)	5126.3(9)	147.3(13)	49.0(5)
C35	1699(3)	5248.1(11)	-764.3(15)	64.2(7)
C36	2348(2)	4873.6(13)	-1253.6(14)	60.7(6)
C37	2977(3)	4370.8(16)	-845.4(16)	74.5(8)
C38	2949(2)	4239.7(11)	64.9(14)	54.9(6)
N1	6812.6(14)	3623.3(7)	2954.5(11)	42.2(4)
O1	1763.7(9)	5024.9(5)	2204.4(7)	25.5(2)
P1	2318.2(3)	4470.40(19)	1758.0(2)	22.88(9)

Table S18. Anisotropic Displacement Parameters ($\text{\AA}^2 \times 10^3$) for **B2**. The Anisotropic displacement factor exponent takes the form: $-2\pi^2[h^2a^{*2}U^{11} + 2hka^{*}b^{*}U^{12} + \dots]$.

Atom	U₁₁	U₂₂	U₃₃	U₁₂	U₁₃	U₂₃
B1	21.2(8)	24.0(8)	25.8(8)	-2.9(6)	3.3(6)	-2.7(6)
C1	31.8(9)	63.8(14)	63.3(13)	15.8(10)	-1.2(9)	-9.2(11)
C2	48.0(12)	42.0(11)	93.2(18)	18.2(10)	0.1(12)	-18.4(12)
C3	26.2(7)	28.9(8)	32.1(8)	4.2(6)	4.8(6)	2.4(6)
C4	23.2(7)	34.9(9)	31.0(8)	-2.7(6)	-0.1(6)	-2.0(6)
C5	26.5(7)	26.5(7)	31.2(8)	-3.4(6)	2.5(6)	-4.6(6)
C6	23.0(7)	23.4(7)	24.5(7)	-1.8(6)	5.7(5)	-0.9(6)
C7	23.4(6)	24.0(7)	25.9(7)	-0.4(6)	4.3(5)	0.2(6)
C8	28.4(7)	25.7(8)	28.9(8)	-0.1(6)	4.5(6)	-3.2(6)
C9	22.5(7)	25.2(7)	26.6(7)	0.8(6)	5.0(6)	0.5(6)
C10	25.4(8)	27.5(7)	28.8(8)	2.0(6)	6.2(6)	3.0(6)
C11	27.1(7)	35.8(8)	30.0(8)	3.3(7)	8.4(6)	5.8(7)
C12	29.1(8)	40.2(9)	26.5(8)	7.6(7)	4.9(6)	-1.2(7)
C13	31.6(8)	31.7(8)	29.3(8)	2.5(7)	2.1(6)	-5.1(6)
C14	25.0(7)	27.4(8)	27.7(7)	1.2(6)	3.6(6)	-1.2(6)
C15	52.1(11)	35.2(9)	41.1(10)	-13.4(8)	20.0(8)	0.8(7)
C16	52.5(12)	58.8(13)	31.9(9)	1.3(10)	16.0(8)	-6.2(9)
C17	33.1(8)	31.3(8)	34.4(8)	-9.4(7)	6.3(6)	-5.4(7)
C18	25.5(7)	22.6(7)	25.6(7)	-2.4(6)	5.3(6)	-2.8(6)
C19	27.8(8)	31.2(8)	31.8(8)	-4.7(6)	8.5(6)	-3.4(6)
C20	33.6(8)	36.7(9)	31.7(8)	-10.5(7)	10.5(7)	1.2(7)
C21	39.7(9)	33.4(9)	29.0(8)	-10.8(7)	1.6(7)	3.1(7)
C22	30.0(8)	28.7(8)	33.4(8)	-0.4(6)	2.2(6)	-0.3(6)
C23	27.2(8)	25.6(7)	26.8(7)	-2.6(6)	5.4(6)	-1.9(6)
C24	25.4(8)	39.4(9)	30.5(8)	6.1(7)	6.2(6)	3.5(7)
C25	50.8(12)	57.6(13)	39.2(10)	-13.6(10)	1.7(8)	16.7(9)
C26	33.2(9)	47.6(11)	54.4(12)	1.8(8)	21.0(8)	11.4(9)
C27	28.5(7)	23.2(7)	26.2(7)	-3.9(6)	4.9(6)	-2.6(6)
C28	37.7(9)	37.3(9)	37.3(9)	-13.1(8)	-3.3(7)	5.7(7)
C29	41.4(10)	52.7(12)	46.8(11)	-22.4(9)	-2.5(8)	3.1(9)
C30	51.2(11)	31.3(9)	49.9(11)	-16.6(8)	14.0(9)	-1.7(8)
C31	56.4(12)	31.0(9)	48.0(11)	-3.9(8)	7.2(9)	10.7(8)
C32	39.5(9)	30.3(9)	38.1(9)	-3.5(7)	-1.8(7)	6.1(7)
C33	29.1(7)	27.1(8)	25.5(7)	-6.1(6)	2.1(6)	-0.7(6)
C34	70.7(14)	38.9(10)	32.5(10)	13.7(10)	-6.0(9)	-3.6(8)
C35	106(2)	40.5(11)	37.2(11)	0.4(12)	-15.1(12)	6.5(9)
C36	77.7(16)	74.4(16)	29.3(10)	-24.9(14)	6.6(10)	8.9(10)

C37	76.4(16)	114(2)	39.1(11)	20.0(17)	27.7(11)	-3.0(14)
C38	63.2(13)	66.0(14)	37.5(10)	26.1(11)	13.7(9)	4.3(9)
N1	32.9(8)	39.4(8)	51.2(9)	13.4(7)	-2.0(7)	-7.0(7)
O1	21.5(5)	26.0(5)	28.7(5)	-1.8(4)	2.9(4)	-3.3(4)
P1	22.90(17)	21.58(17)	23.63(17)	-2.31(15)	2.23(12)	-1.15(14)

Table S19. Bond Lengths for **B2**.

Atom	Atom	Length/Å	Atom	Atom	Length/Å
B1	C6	1.629(2)	C19	C20	1.402(2)
B1	C9	1.635(2)	C19	C26	1.507(3)
B1	C18	1.647(2)	C20	C21	1.377(3)
B1	O1	1.6434(19)	C21	C22	1.382(2)
C1	N1	1.439(3)	C21	C25	1.518(2)
C2	N1	1.434(3)	C22	C23	1.393(2)
C3	C4	1.406(2)	C23	C24	1.509(2)
C3	C8	1.399(2)	C27	C28	1.394(2)
C3	N1	1.386(2)	C27	C32	1.389(2)
C4	C5	1.377(2)	C27	P1	1.7894(16)
C5	C6	1.407(2)	C28	C29	1.384(2)
C6	C7	1.402(2)	C29	C30	1.378(3)
C7	C8	1.397(2)	C30	C31	1.368(3)
C7	P1	1.7715(14)	C31	C32	1.395(3)
C9	C10	1.419(2)	C33	C34	1.377(2)
C9	C14	1.410(2)	C33	C38	1.382(3)
C10	C11	1.393(2)	C33	P1	1.7932(16)
C10	C15	1.506(2)	C34	C35	1.384(3)
C11	C12	1.381(2)	C35	C36	1.359(4)
C12	C13	1.380(2)	C36	C37	1.366(4)
C12	C16	1.505(2)	C37	C38	1.386(3)
C13	C14	1.398(2)	O1	P1	1.5325(11)
C14	C17	1.514(2)			
C18	C19	1.416(2)			
C18	C23	1.421(2)			

Table S20. Bond Angles for **B2**.

Atom	Atom	Atom	Angle/°	Atom	Atom	Atom	Angle/°
C9	B1	C6	108.65(12)	C26	C19	C20	115.31(14)
C18	B1	C6	118.89(12)	C21	C20	C19	122.81(14)
C18	B1	C9	117.80(13)	C22	C21	C20	117.05(15)

O1	B1	C6	99.57(11)	C25	C21	C20	121.28(16)
O1	B1	C9	111.15(11)	C25	C21	C22	121.67(17)
O1	B1	C18	98.44(11)	C23	C22	C21	122.41(15)
C8	C3	C4	117.30(14)	C22	C23	C18	121.06(13)
N1	C3	C4	121.32(15)	C24	C23	C18	121.92(14)
N1	C3	C8	121.37(15)	C24	C23	C22	117.03(14)
C5	C4	C3	122.34(14)	C32	C27	C28	119.58(15)
C6	C5	C4	122.02(14)	P1	C27	C28	119.27(12)
C5	C6	B1	129.20(13)	P1	C27	C32	121.05(12)
C7	C6	B1	116.36(13)	C29	C28	C27	119.53(17)
C7	C6	C5	114.40(13)	C30	C29	C28	120.68(17)
C8	C7	C6	124.84(13)	C31	C30	C29	120.16(16)
P1	C7	C6	106.11(11)	C32	C31	C30	120.21(17)
P1	C7	C8	129.04(12)	C31	C32	C27	119.82(16)
C7	C8	C3	118.90(14)	C38	C33	C34	118.93(17)
C10	C9	B1	123.92(13)	P1	C33	C34	120.85(13)
C14	C9	B1	119.67(13)	P1	C33	C38	120.14(14)
C14	C9	C10	116.22(14)	C35	C34	C33	120.1(2)
C11	C10	C9	120.42(15)	C36	C35	C34	120.7(2)
C15	C10	C9	123.26(14)	C37	C36	C35	119.89(19)
C15	C10	C11	116.29(14)	C38	C37	C36	120.1(2)
C12	C11	C10	122.94(15)	C37	C38	C33	120.3(2)
C13	C12	C11	117.00(14)	C2	N1	C1	119.01(16)
C16	C12	C11	120.40(16)	C3	N1	C1	120.82(16)
C16	C12	C13	122.58(16)	C3	N1	C2	120.15(16)
C14	C13	C12	121.99(15)	P1	O1	B1	111.70(8)
C13	C14	C9	121.37(14)	C27	P1	C7	112.75(7)
C17	C14	C9	122.69(14)	C33	P1	C7	112.40(7)
C17	C14	C13	115.94(14)	C33	P1	C27	107.42(7)
C19	C18	B1	125.56(14)	O1	P1	C7	101.97(7)
C23	C18	B1	117.67(12)	O1	P1	C27	112.08(6)
C23	C18	C19	116.14(14)	O1	P1	C33	110.25(7)
C20	C19	C18	120.50(15)				
C26	C19	C18	124.18(15)				

Table S21. Hydrogen Atom Coordinates ($\text{\AA} \times 10^4$) and Isotropic Displacement Parameters ($\text{\AA}^2 \times 10^3$) for **B2**.

Atom	x	y	z	U(eq)
H1a	8324.6	4144.4	3273	81
H1b	8587.1	3408.1	3326.6	81

H1c	7990	3746	4111.5	81
H2a	5910	2817.3	2733.9	94
H2b	7316.4	2780.9	2582.4	94
H2c	6308.6	3113.1	1835.9	94
H4	6801.4	4657.4	3885.7	36
H5	5287.6	5398.8	3862.5	34
H8	4572	3620.3	2009.3	33
H11	1142.4	5243.7	5447.3	37
H13	3227	6767.2	5322.7	37
H15a	639.2	4751.8	3398.9	62
H15b	902.8	4489.7	4421.4	62
H15c	1920.6	4413.3	3771.9	62
H16a	2712.3	6193.4	6905.7	70
H16b	1344	5916.5	6682.7	70
H16c	1592.7	6635.7	6476.1	70
H17a	4480.7	6418.5	3473.7	49
H17b	4296	6951.5	4195.7	49
H17c	3358.7	6900.8	3253.7	49
H20	4068.9	6619.1	295.6	40
H22	723.8	7009	877.3	37
H24a	924.4	6518.1	2919.3	47
H24b	440.6	5894.4	2381.7	47
H24c	-75.9	6561.5	2009.1	47
H25a	1776.7	7063.6	-921.4	75
H25b	2891.9	7502.4	-473	75
H25c	1526.4	7632.2	-275.2	75
H26a	5336.4	5896	2174.6	65
H26b	5443.2	6031.8	1130.7	65
H26c	4845.8	5391.2	1405.2	65
H28	51	3975.2	836.1	46
H29	-1074.5	3065.8	975.2	58
H30	-362.9	2326.7	2081.9	52
H31	1493.2	2478.3	3044.6	54
H32	2663.4	3380.2	2907.8	44
H34	1216.2	5393.1	483.7	59
H35	1263.9	5597.3	-1051.2	77
H36	2363.1	4960.9	-1879.4	73
H37	3436.9	4111	-1185.2	89
H38	3381.1	3887.3	344.3	66

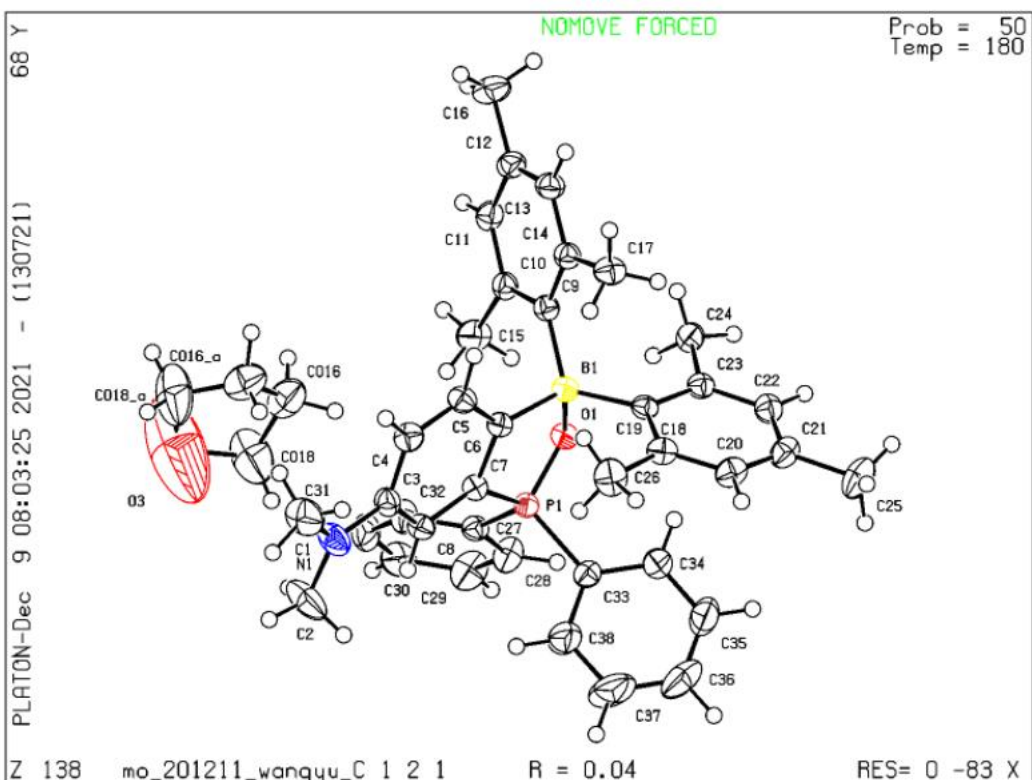


Figure S49. Crystal structure of **B2**.

Table S22. Crystal data and structure refinement for **B3**.

Identification code	B3
Empirical formula	C ₃₈ H ₄₁ BNO ₃ P
Formula weight	601.53
Temperature/K	180.0
Crystal system	triclinic
Space group	P-1
a/Å	12.1030(5)
b/Å	12.3409(7)
c/Å	13.4164(8)
α/°	88.811(2)
β/°	71.353(2)
γ/°	75.150(2)
Volume/Å ³	1831.19(17)
Z	2
ρ _{calcd} /cm ³	1.222
μ/mm ⁻¹	0.118
F(000)	720.0

Crystal size/mm ³	0.38 × 0.34 × 0.14
Radiation	MoKα ($\lambda = 0.71073$)
2Θ range for data collection/°	4.766 to 55.006
Index ranges	-15 ≤ h ≤ 15, -15 ≤ k ≤ 16, -17 ≤ l ≤ 14
Reflections collected	21989
Independent reflections	8359 [R _{int} = 0.0322, R _{sigma} = 0.0438]
Data/restraints/parameters	8359/0/450
Goodness-of-fit on F ²	1.045
Final R indexes [I>=2σ (I)]	R ₁ = 0.0462, wR ₂ = 0.1198
Final R indexes [all data]	R ₁ = 0.0671, wR ₂ = 0.1320
Largest diff. peak/hole / e Å ⁻³	0.33/-0.36

Table S23. Fractional Atomic Coordinates ($\times 10^4$) and Equivalent Isotropic Displacement Parameters ($\text{Å}^2 \times 10^3$) for **B3**. Ueq is defined as 1/3 of the trace of the orthogonalised U_{II} tensor.

Atom	x	y	z	U(eq)
B1	6518.4(14)	7239.2(15)	5795.1(13)	21.4(3)
C1	10573.3(17)	4856.1(19)	1214.7(16)	47.7(5)
C2	8710.7(15)	5784.4(14)	2511.2(13)	29.8(4)
C3	7457.0(15)	6066.7(15)	2818.6(13)	32.7(4)
C4	6749.9(14)	6492.9(15)	3832.3(13)	29.5(4)
C5	5396.5(16)	6704(2)	4076.2(17)	54.1(6)
C6	7276.8(13)	6696.2(13)	4593.1(12)	22.8(3)
C7	8549.7(13)	6376.1(13)	4263.8(12)	23.7(3)
C8	9255.0(14)	5921.6(14)	3241.0(12)	27.2(3)
C9	9255.5(14)	6513.4(15)	4986.0(13)	29.0(4)
C10	8686(2)	11605.8(18)	6211.5(18)	54.0(6)
C11	7817.4(14)	10061.3(14)	6684.2(13)	28.2(3)
C12	7660.4(13)	9212.0(14)	7364.4(12)	26.0(3)
C13	7554.9(15)	10022.5(14)	5759.3(13)	29.4(4)
C14	7279.3(12)	8310.6(13)	7117.1(12)	22.7(3)
C15	7167.8(16)	7440.3(15)	7929.8(13)	31.5(4)
C16	7025.9(12)	8229.8(13)	6164.1(12)	21.4(3)
C17	6862.4(17)	9210.5(15)	4484.6(14)	34.3(4)
C18	7155.7(13)	9135.3(14)	5507.4(12)	24.9(3)
C19	6202.8(13)	6266.6(13)	6594.4(12)	21.6(3)
C20	6925.2(14)	5204.9(13)	6681.8(13)	26.6(3)
C21	5012.6(13)	6502.0(13)	7289.7(12)	21.4(3)
C22	4554.7(14)	5801.7(14)	8047.6(12)	26.3(3)

C23	6506.2(15)	4486.7(14)	7429.1(14)	30.4(4)
C24	5314.6(15)	4763.7(14)	8141.1(13)	29.6(4)
C25	5716.6(19)	2978.1(16)	8961.1(18)	47.5(5)
C26	3732.4(17)	4363.4(17)	9652.8(15)	41.3(5)
C27	3971.5(13)	8928.8(13)	7916.7(13)	24.7(3)
C28	4338.0(15)	9896.0(15)	7600.0(15)	32.9(4)
C29	4197.3(18)	10719.8(18)	8348.7(18)	47.2(5)
C30	3714(2)	10568.5(19)	9408.8(19)	54.6(6)
C31	3336(2)	9618.3(19)	9731.5(17)	51.6(5)
C32	3453.6(17)	8795.3(16)	8989.3(14)	37.7(4)
C33	2820.5(13)	7765.5(13)	6847.3(12)	22.5(3)
C34	1840.1(13)	8715.4(14)	7110.8(13)	27.2(3)
C35	762.5(15)	8664.9(16)	6979.2(14)	33.9(4)
C36	661.2(15)	7678.7(16)	6597.4(14)	35.4(4)
C37	1634.5(15)	6730.8(15)	6331.6(14)	33.1(4)
C38	2712.3(14)	6774.1(14)	6461.4(13)	28.8(4)
N1	4910.7(15)	4022.9(14)	8865.2(14)	50.3(5)
O1	8231.4(12)	10896.3(11)	7002.1(10)	39.0(3)
O2	9317.8(11)	5356.0(12)	1481.8(9)	41.6(3)
O3	5139.8(9)	7966.9(9)	5905.9(8)	21.9(2)
P1	4236.9(3)	7813.9(3)	6964.7(3)	20.19(11)

Table S24. Anisotropic Displacement Parameters ($\text{\AA}^2 \times 10^3$) for **B3**. The Anisotropic displacement factor exponent takes the form: $-2\pi^2[h^2a^{*2}U^{11} + 2hka^{*}b^{*}U^{12} + \dots]$.

Atom	U ₁₁	U ₂₂	U ₃₃	U ₂₃	U ₁₃	U ₁₂
B1	17.4(7)	25.7(9)	21.2(8)	1.1(7)	-7.1(6)	-5.0(7)
C1	38.3(10)	61.0(14)	29.4(10)	-13.2(9)	-0.4(8)	-0.5(9)
C2	33.5(8)	32.1(9)	19.0(8)	-1.2(7)	-4.2(6)	-5.9(7)
C3	34.9(9)	41.8(10)	23.9(9)	-4.8(7)	-12.9(7)	-9.5(8)
C4	25.8(8)	37.9(10)	25.9(8)	-3.2(7)	-8.5(6)	-9.7(7)
C5	28.2(9)	96.2(18)	39.2(11)	-27.3(11)	-11.5(8)	-15.6(11)
C6	22.8(7)	26.7(8)	19.9(8)	2.1(6)	-6.0(6)	-9.6(6)
C7	24.2(7)	25.8(8)	22.4(8)	2.5(6)	-7.4(6)	-9.3(6)
C8	22.7(7)	32.1(9)	23.6(8)	1.3(7)	-2.6(6)	-8.1(7)
C9	19.4(7)	38.3(9)	28.5(9)	-2.9(7)	-7.3(6)	-6.3(7)
C10	73.4(15)	44.2(12)	53.8(13)	0.3(10)	-16.5(11)	-36.8(11)
C11	23.4(7)	27.9(8)	32.8(9)	-6.2(7)	-7.8(6)	-7.4(6)
C12	20.5(7)	35.2(9)	22.2(8)	-5.8(7)	-7.5(6)	-5.7(6)
C13	30.1(8)	28.5(9)	30.0(9)	4.4(7)	-8.7(7)	-10.3(7)

C14	16.2(7)	28.5(8)	21.7(8)	-0.9(6)	-5.6(6)	-3.5(6)
C15	36.2(9)	41.7(10)	24.0(8)	5.6(7)	-16.9(7)	-14.3(8)
C16	16.3(6)	26.2(8)	21.4(8)	-0.8(6)	-6.0(6)	-5.1(6)
C17	46.2(10)	37.2(10)	29.4(9)	11.7(8)	-19.7(8)	-19.4(8)
C18	23.0(7)	29.6(8)	22.8(8)	1.8(7)	-8.2(6)	-7.0(6)
C19	20.9(7)	25.0(8)	19.6(7)	-1.8(6)	-7.1(6)	-6.1(6)
C20	20.0(7)	28.3(8)	27.7(8)	-0.4(7)	-5.5(6)	-2.6(6)
C21	20.1(7)	22.7(8)	21.1(7)	0.2(6)	-7.2(6)	-4.4(6)
C22	21.5(7)	31.0(9)	24.4(8)	3.0(7)	-5.3(6)	-6.5(6)
C23	28.8(8)	25.3(8)	35.0(9)	3.8(7)	-11.9(7)	-2.0(7)
C24	30.8(8)	30.7(9)	27.7(9)	8.1(7)	-9.7(7)	-8.8(7)
C25	51.0(12)	35.7(11)	59.7(14)	22.2(10)	-21.6(10)	-15.0(9)
C26	45.8(11)	46.9(11)	31.2(10)	14.5(9)	-8.5(8)	-18.5(9)
C27	20.8(7)	26.8(8)	26.6(8)	-2.7(6)	-11.2(6)	-1.7(6)
C28	29.0(8)	32.3(9)	38.2(10)	-3.4(8)	-11.0(7)	-8.8(7)
C29	44.3(11)	38.8(11)	58.6(14)	-14.0(10)	-13.8(10)	-13.5(9)
C30	56.1(13)	51.2(13)	54.0(14)	-26.7(11)	-18.8(11)	-6.4(11)
C31	62.5(13)	53.2(13)	31.0(11)	-12.3(9)	-12.3(10)	-3.7(11)
C32	44.4(10)	35.5(10)	28.4(9)	-2.4(8)	-9.5(8)	-5.2(8)
C33	19.7(7)	26.6(8)	22.0(8)	3.3(6)	-7.1(6)	-7.3(6)
C34	22.9(7)	28.2(8)	30.7(9)	0.2(7)	-9.4(6)	-6.0(6)
C35	21.6(8)	39.8(10)	39.1(10)	1.8(8)	-12.3(7)	-2.9(7)
C36	23.6(8)	50.3(11)	37.5(10)	1.7(8)	-13.9(7)	-13.5(8)
C37	33.2(9)	37.2(10)	35.1(10)	0.5(8)	-13.1(7)	-17.2(8)
C38	26.2(8)	29.1(9)	31.8(9)	0.9(7)	-10.0(7)	-7.6(7)
N1	42.1(9)	42.3(10)	51.6(11)	26.7(8)	-2.5(8)	-3.8(8)
O1	46.5(7)	37.1(7)	40.2(7)	-4.1(6)	-15.3(6)	-20.8(6)
O2	39.1(7)	55.5(8)	21.2(6)	-7.9(6)	-4.4(5)	-3.2(6)
O3	18.4(5)	26.6(6)	21.7(5)	4.1(4)	-7.9(4)	-6.1(4)
P1	17.05(18)	23.0(2)	20.7(2)	1.25(15)	-6.87(14)	-4.55(15)

Table S25. Bond Lengths for **B3**.

Atom	Atom	Length/Å	Atom	Atom	Length/Å
B1	C6	1.636(2)	C21	C22	1.392(2)
B1	C16	1.650(2)	C21	P1	1.7737(15)
B1	C19	1.630(2)	C22	C24	1.402(2)
B1	O3	1.6406(18)	C23	C24	1.410(2)
C1	O2	1.414(2)	C24	N1	1.381(2)
C2	C3	1.389(2)	C25	N1	1.435(2)

C2	C8	1.378(2)	C26	N1	1.440(2)
C2	O2	1.382(2)	C27	C28	1.390(2)
C3	C4	1.383(2)	C27	C32	1.399(2)
C4	C5	1.517(2)	C27	P1	1.7921(17)
C4	C6	1.421(2)	C28	C29	1.384(3)
C6	C7	1.409(2)	C29	C30	1.383(3)
C7	C8	1.401(2)	C30	C31	1.378(3)
C7	C9	1.519(2)	C31	C32	1.386(3)
C10	O1	1.425(2)	C33	C34	1.394(2)
C11	C12	1.385(2)	C33	C38	1.391(2)
C11	C13	1.380(2)	C33	P1	1.7868(15)
C11	O1	1.3836(19)	C34	C35	1.388(2)
C12	C14	1.391(2)	C35	C36	1.379(3)
C13	C18	1.392(2)	C36	C37	1.388(3)
C14	C15	1.514(2)	C37	C38	1.384(2)
C14	C16	1.418(2)	O3	P1	1.5328(10)
C16	C18	1.418(2)			
C17	C18	1.519(2)			
C19	C20	1.403(2)			
C19	C21	1.402(2)			
C20	C23	1.384(2)			

Table S26. Bond Angles for **B3**.

Atom	Atom	Atom	Angle/ [°]	Atom	Atom	Atom	Angle/ [°]
C6	B1	C16	113.85(12)	C22	C21	P1	128.31(12)
C6	B1	O3	111.96(11)	C21	C22	C24	119.16(14)
C19	B1	C6	111.01(13)	C20	C23	C24	122.24(15)
C19	B1	C16	119.27(12)	C22	C24	C23	116.81(14)
C19	B1	O3	99.25(10)	N1	C24	C22	122.01(15)
O3	B1	C16	99.72(11)	N1	C24	C23	121.13(15)
C8	C2	C3	118.86(15)	C28	C27	C32	119.93(16)
C8	C2	O2	124.99(15)	C28	C27	P1	120.38(13)
O2	C2	C3	116.13(15)	C32	C27	P1	119.59(13)
C4	C3	C2	121.49(15)	C29	C28	C27	119.80(18)
C3	C4	C5	115.86(15)	C30	C29	C28	119.9(2)
C3	C4	C6	121.30(15)	C31	C30	C29	120.7(2)
C6	C4	C5	122.83(15)	C30	C31	C32	119.9(2)
C4	C6	B1	124.93(13)	C31	C32	C27	119.66(18)
C7	C6	B1	119.34(13)	C34	C33	P1	120.75(12)

C7	C6	C4	115.72(14)	C38	C33	C34	119.99(14)
C6	C7	C9	122.46(14)	C38	C33	P1	119.24(12)
C8	C7	C6	122.30(14)	C35	C34	C33	119.56(16)
C8	C7	C9	115.24(13)	C36	C35	C34	120.14(16)
C2	C8	C7	120.23(15)	C35	C36	C37	120.59(15)
C13	C11	C12	118.95(15)	C38	C37	C36	119.62(16)
C13	C11	O1	125.05(15)	C37	C38	C33	120.10(15)
O1	C11	C12	116.01(15)	C24	N1	C25	120.79(16)
C11	C12	C14	121.27(14)	C24	N1	C26	120.22(15)
C11	C13	C18	120.49(15)	C25	N1	C26	118.21(15)
C12	C14	C15	115.18(14)	C11	O1	C10	116.31(14)
C12	C14	C16	121.37(14)	C2	O2	C1	116.84(14)
C16	C14	C15	123.45(14)	P1	O3	B1	111.22(8)
C14	C16	B1	126.41(13)	C21	P1	C27	112.17(7)
C14	C16	C18	115.63(14)	C21	P1	C33	111.59(7)
C18	C16	B1	117.84(13)	C33	P1	C27	108.62(7)
C13	C18	C16	122.24(14)	O3	P1	C21	101.27(6)
C13	C18	C17	115.27(14)	O3	P1	C27	110.88(7)
C16	C18	C17	122.49(14)	O3	P1	C33	112.22(6)
C20	C19	B1	130.26(13)				
C21	C19	B1	115.72(13)				
C21	C19	C20	113.99(13)				
C23	C20	C19	122.35(14)				
C19	C21	P1	106.29(11)				
C22	C21	C19	125.35(14)				

Table S27. Hydrogen Atom Coordinates ($\text{\AA} \times 10^4$) and Isotropic Displacement Parameters ($\text{\AA}^2 \times 10^3$) for **B3**.

Atom	x	y	z	U(eq)
H1A	10894.79	4547.26	480.98	72
H1B	10715.6	4250.86	1679.83	72
H1C	10979.77	5423.7	1298.24	72
H3	7076.38	5964.91	2321.38	39
H5A	5064.02	6336.11	4715.35	81
H5B	5235.24	6398.52	3484.23	81
H5C	5015.63	7514.37	4186.63	81
H8	10111.4	5707.46	3050.15	33
H9A	9303.58	7292.97	5005.78	44
H9B	10073.12	6010.39	4719.71	44

H9C	8845.28	6325.37	5698.48	44
H10A	9292.69	11143.4	5598.05	81
H10B	9057.59	12091.82	6492.79	81
H10C	8020.8	12070.29	5999.89	81
H12	7815.95	9245.49	8012.15	31
H13	7647.46	10605.72	5291.19	35
H15A	6313.67	7462.41	8264.69	47
H15B	7504.82	7602.99	8466.29	47
H15C	7612.87	6692.24	7584.43	47
H17A	7558.67	8767.05	3916.73	51
H17B	6678.31	9996.86	4308.55	51
H17C	6161.02	8916.24	4568.47	51
H20	7730.97	4970.12	6211.26	32
H22	3737.62	6024.2	8495.93	32
H23	7039.44	3783.23	7463.51	36
H25A	6036.51	2527.55	8288.46	71
H25B	5277.39	2566.17	9513.01	71
H25C	6386.1	3126.9	9147.23	71
H26A	3668.06	5042.83	10056.16	62
H26B	3616.36	3759.8	10129.67	62
H26C	3111.15	4519.31	9308.29	62
H28	4683.95	9991.48	6871.81	40
H29	4432.26	11388.46	8134.64	57
H30	3642.61	11125.84	9920.35	66
H31	2995.68	9527.64	10461.42	62
H32	3183.71	8143.92	9207.81	45
H34	1909.23	9392.71	7378.73	33
H35	93.2	9311.18	7152.6	41
H36	-81.62	7647.92	6515.53	42
H37	1561.61	6056.01	6062.13	40
H38	3379.07	6125.54	6286.68	35

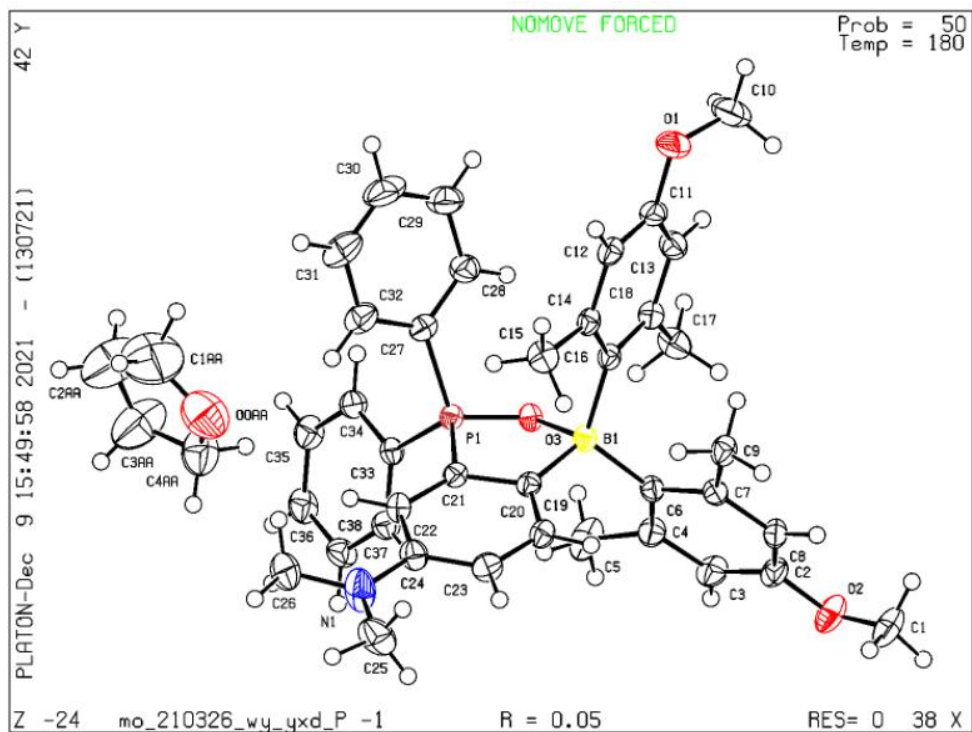


Figure S50. Crystal structure of **B3**.

Reference

1. C. Fischer and C. Sparr, Angewandte Chemie International Edition, 2018, 57, 2436-2440.
2. M.J. Frisch, G. W. Trucks, H. B. Schlegel, G. E. Scuseria, M. A. Robb, J. R. Cheeseman, G. Scalmani, V. Barone, B. Mennucci, G. A. Petersson, H. Nakatsuji, M. Caricato, X. Li, H. P. Hratchian, A. F. Izmaylov, J. Bloino, G. Zheng, J. L. Sonnenberg, M. Hada, M. Ehara, K. Toyota, R. Fukuda, J. Hasegawa, M. Ishida, T. Nakajima, Y. Honda, O. Kitao, H. Nakai, T. Vreven, J. A. Montgomery, J. E. Peralta, F. Ogliaro, M. J. Bearpark, J. Heyd, E. N. Brothers, K. N. Kudin, V. N. Staroverov, R. Kobayashi, J. Normand, K. Raghavachari, A. P. Rendell, J. C. Burant, S. S. Iyengar, J. Tomasi, M. Cossi, N. Rega, N. J. Millam, M. Klene, J. E. Knox, J. B. Cross, V. Bakken, C. Adamo, J. Jaramillo, R. Gomperts, R. E. Stratmann, O. Yazyev, A. J. Austin, R. Cammi, C. Pomelli, J. W. Ochterski, R. L. Martin, K. Morokuma, V. G. Zakrzewski, G. A. Voth, P. Salvador, J. J. Dannenberg, S. Dapprich, A. D. Daniels, Ö. Farkas, J. B. Foresman, J. V. Ortiz, J. Cioslowski, D. J. Fox, Gaussian 09 Revision C.01, 2010.
3. a) C. Lee, W. Yang and R. G. Parr, Physical Review B, 1988, 37, 785-789. b) A. D. Becke, The Journal of Chemical Physics, 1993, 98, 1372-1377. c) A. D. Becke, The Journal of Chemical Physics, 1993, 98, 5648-5652. d) R. Ditchfield, W. J. Hehre and J. A. Pople, The Journal of Chemical Physics, 1971, 54, 724-728. e) A. D. McLean and G. S. Chandler, The Journal of Chemical Physics, 1980, 72, 5639-5648.
4. O. V. Dolomanov, L. J. Bourhis, R. J. Gildea, J. A. K. Howard and H. Puschmann, Journal of Applied Crystallography, 2009, 42, 339-341.
5. G.M. Sheldrick, (1997) SHELXL-97: Program for the Refinement of Crystal Structures. University of Göttingen, Germany.